Research Square

Preprints are preliminary reports that have not undergone peer review.
They should not be considered conclusive, used to inform clinical practice,
or referenced by the media as validated information.

End value formulations for mitigating finite-horizon distortions in Ramsey-based integrated assessment models

Joanna Sitarz

joanna.sitarz@pik-potsdam.de

Potsdam Institute for Climate Impact Research

Robert Pietzcker

Potsdam Institute for Climate Impact Research

Gunnar Luderer

Potsdam Institute for Climate Impact Research

Research Article

Keywords:

Posted Date: November 18th, 2026

DOI: https://doi.org/10.21203/rs.3.rs-11445639/v1

License: This work is licensed under a Creative Commons Attribution 4.0 International License.
Read Full License

Additional Declarations: No competing interests reported.

End value formulations for mitigating finite-horizon distortions in Ramsey-based integrated assessment models

Joanna Sitarz[1,2*], Robert Pietzcker[1] and Gunnar Luderer[1,2]

[1]Energy Transition Lab, Potsdam Institute for Climate Impact Research, Potsdam, Germany.
[2]Global Energy Systems Analysis, Technische Universität Berlin, Berlin, Germany.

*Corresponding author(s). E-mail(s): joanna.sitarz@pik-potsdam.de;

Abstract

Approximating infinite-horizon problems with finite-horizon optimization is a persistent challenge in Ramsey-type integrated assessment models (IAMs), often leading to end-of-horizon distortions. As the end of the optimization horizon approaches, the social planner has no incentive to invest and instead consumes all output. Extending the optimization horizon, a common practice in numerically solved IAMs, can mitigate these terminal effects but increases computational costs and is unsuitable for deliberately myopic models. An alternative is to add an end value, representing the value of remaining stocks, to the objective function. However, existing formulations have been limited to simple Ramsey growth models. This article proposes two approaches for formulating end values, applicable to both standard Ramsey growth models and hybrid energy-economy models. The first approach employs an explicit integrated tail of future utility flows, while the second uses an iterative algorithm based on shadow prices. Using a nonlinear programming framework, we evaluate both formulations across varying horizon lengths. The results demonstrate that while both approaches converge to the infinite-horizon solution over sufficiently long horizons, shorter horizons reveal distinct behaviors. These differences do not represent errors, but rather reflect alternative assumptions about how the social planner treats the post-horizon future. Consequently, the end-value choice should be treated as a deliberate modeling decision tailored to the specific case study.

Keywords: Integrated Assessment Model, Ramsey growth model, nonlinear optimization, infinite horizon approximation, end value, terminal value, end effects

1 Introduction

Climate change is one of the most complex issues confronting humanity today, encompassing multiple dimensions as natural sciences, economics, policy, and social factors. Although discipline-specific research advances knowledge in distinct areas, a field that synthesizes insights across multiple domains is essential for developing comprehensive solutions. Integrated Assessment Modelling (IAM) has gradually emerged as one of the most powerful tools in this domain. By combining economic modeling with energy systems and climate modeling, IAMs have evolved from the early approaches pioneered by Nordhaus (1992a) into the computational backbone of scientific support for policy decision-making, serving, e.g., as key tools for exploring mitigation scenarios in multiple IPCC reports (Weyant, 2017).

Although there is no single definition of an IAM, many are global in scope and include both an economic description and a representation of processes that produce greenhouse gas (GHG) emissions (Fisher-Vanden and Weyant, 2020; Weyant, 2017). While simple IAMs can be solved analytically, more complex models, particularly "detailed-process IAMs" (Weyant, 2017), such as those developed by teams within the Integrated Assessment Modeling Consortium (IAMC), require numerical methods.

Many IAMs incorporate economic growth models to represent long-term dynamics, typically following either the Ramsey or Solow framework (Guivarch et al., 2022). Ramsey-based IAMs, which have an endogenous savings rate, are social planner problems maximizing welfare by optimizing decisions on investment versus consumption over a given time horizon. A common approach to solving IAM social planner problems numerically is to formulate them as nonlinear optimization problems. Prominent IAM examples in that category include DICE (Nordhaus, 1992b), MERGE (Manne et al., 1995), WITCH (Bosetti et al., 2007), or REMIND (Luderer et al., 2015).

1.1 Problem statement

A particular challenge faced by Ramsey-based IAMs formulated as optimization problems lies in approximating the infinite horizon (as in the original Ramsey growth model) with a finite optimization horizon, which is necessary to make the problem computationally feasible. This approximation of the economy gives rise to unwanted end effects. In the final time steps, the social planner has no incentive to invest and would consume all generated output.

The literature presents different approaches to handle the approximation of the infinite horizon in Ramsey-type problems. One widely used approach (e.g., in DICE and REMIND) involves extending the optimization horizon to postpone the end effects beyond the period of interest. However, this approach increases computational complexity by adding additional time steps and is not suitable for myopic models, where the foresight horizon is kept short on purpose to realistically depict a planning agent with limited foresight.

An alternative solution involves formulating an end value and adding it to the objective function. The end value[1] refers to the value that the remaining stocks (e.g. capital, resources) still have for the future of the economy at the end of the optimization horizon.

To the best of our knowledge, end-value formulations for the approximation of infinite-horizon problems have only focused on simple Ramsey-type growth models and did not include formulations suitable for more complex IAMs, i.e., in which an economic module is coupled to a detailed description of the energy sector. Such hybrid energy-economy models—hereafter referred to simply as hybrid models—typically involve not only the macroeconomic capital stock but also other stock variables, such as energy generation capacities.

1.2 Research contribution

Our study closes this research gap by proposing two approaches for formulating end values to minimize end effects in hybrid models. Approach 1, an explicit end value using an integrated tail, extends existing formulations for Ramsey-type models. In this approach, the end value captures the sum of all future utility flows beyond the end of the horizon. Approach 2 is an iterative approach based on shadow prices. In this case,the end value equals the standing capital at the end of the horizon multiplied by its shadow price (representing the utility value of this capital stock). We formulate both a simple Ramsey growth model and a hybrid model in GAMS (GAMS Development Corporation, 2025) as nonlinear programs to test the performance of both methods. To do so, we vary the horizon length and chosen parameters, comparing the results to a model with a significantly longer foresight that acts as a numerical substitute for an infinite-horizon solution.

The article is structured as follows: Section 2 describes the problem of end effects illustrated using the Ramsey growth model, and presents various solution approaches from the literature. Section 3 introduces our model used for the experiments and then presents our contribution: two methods for formulating an end value in a hybrid model. Section 4 discusses results for both approaches, first for the pure Ramsey growth model and subsequently for the hybrid model. Section 5 concludes with final remarks.

2 Background

This section first introduces the Ramsey growth model and discusses the problems arising from approximating an infinite horizon with a finite horizon. It then presents different approaches to mitigate end effects found in the literature.

[1] In the literature, the term *end value* is used interchangeably with *terminal value, terminal cost, or salvage value*; Throughout this article we will use *end value*.

2.1 Ramsey growth model

In the Ramsey growth model (Ramsey, 1928), a social planner seeks to maximize the welfare function

$$\int_{t=0}^{\infty} U(C(t))\, e^{-\theta t} dt \tag{2.1}$$

representing the sum of utility $U(C(t))$ over an *infinite* horizon, discounted by the pure rate of time preference θ, subject to the budget constraint

$$Y(t) = C(t) + I(t). \tag{2.2}$$

Therein, $C(t)$ is the consumption at time t, $I(t)$ the investment, and $Y(t)$ the output defined by a production function, e.g, a CES function

$$Y(t) = A(t) \left[\xi_K (\mu_K K(t))^{\rho} + \xi_L (\mu_L L(t))^{\rho}\right]^{\frac{1}{\rho}} \tag{2.3}$$

with $A(t)$ the total productivity factor, ξ the share parameters, μ the efficiency parameters, and ρ the substitution parameter. The evolution of the capital stock $K(t)$ is described by

$$\dot{K}(t) = I(t) - \delta K(t), \tag{2.4}$$

whereas δ denotes the capital depreciation rate. Labor is assumed to grow at a constant rate n, s.t.

$$L(t) = L_0 e^{nt}. \tag{2.5}$$

2.2 The finite-horizon problem

To solve the Ramsey growth model numerically, it must be discretized over time, and the *infinite* horizon needs to be approximated by a *finite* horizon. The model can then be formulated as a nonlinear program (2.6) - (2.11) with T denoting the final time step of the optimization horizon. For simplicity reasons, we assume throughout this article $\Delta t = 1$.

$$\max_{\{C_t\}} \quad \sum_{t=0}^{T} U(C_t) e^{-\theta t} \tag{2.6}$$

$$\begin{aligned}
\text{s.t.} \quad & Y_t = C_t + I_t && (2.7)\\
\forall t \in \{0,..,T\} \quad & Y_t = f(K_t, L_t) = A_t \left[\xi_K (\mu_K K_t)^\rho + \xi_L (\mu_L L_t)^\rho\right]^{\frac{1}{\rho}} && (2.8)\\
& L_t = L_0 e^{nt} && (2.9)\\
& K_{t+1} = K_t(1-\delta) + I_t && (2.10)\\
& I_t \geq 0 && (2.11)\\
& \text{with } K_0 > 0 \text{ and } L_0 > 0 \text{ given.}
\end{aligned}$$

Figure 1 shows the solution of the Ramsey problem formulated as a finite-horizon nonlinear optimization problem, where the final time step $t = T$ is set 2100. Here, and throughout this study, we show results for the case of a non-growing economy. This simplification is made strictly for visual clarity when illustrating the evolution of variables and the resulting end effects. This assumption does not affect any methods or conclusions drawn in this work. Additional results for the case of a growing economy are provided in Appendix G.

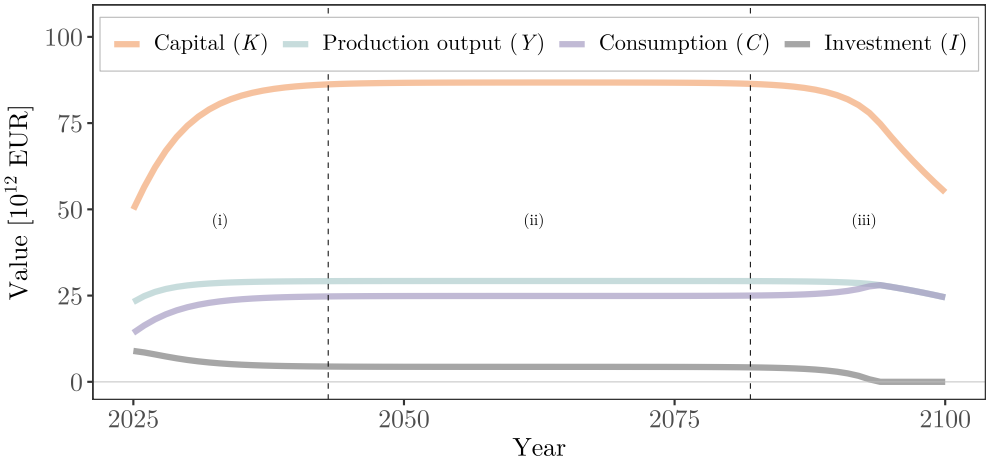


Fig. 1: | **Evolution of variables K, Y, C, and I in a Ramsey model formulated as finite-horizon nonlinear optimization problem.** We distinguish three phases: (i) transition, (ii) steady state, and (iii) end effects. We set the initial year $t = 0$ to 2025 and final $t = T$ to 2100. We assume logarithmic utility $U(C_t) = \ln(C_t)$, a constant total productivity factor $A_t = A$, and $n = 0$, s.t., $L_t = L_0, \forall t \in \{0, \dots, T\}$. Details of the parametrization are provided in Appendix E.

Overall, the evolution of the economy can be described by three phases: (i) *transition*, (ii) *steady state*, and (iii) *end effects*. In the *transition phase*, the economy moves from an initial state toward a balanced growth path - here *steady-state* as for simplicity reasons we assume constant labor $L_t = L_0$. As the optimization horizon nears its end ($t = T$), *end effects* emerge. In this phase, the model prioritizes consumption over investments, as it no longer accounts for the future beyond the optimization horizon, resulting in investments I falling to zero by 2100. Consequently, the entire production output Y is consumed, causing the lines for C and Y to overlap. As a result, capital K is significantly reduced toward the end of the horizon.

2.3 Approaches to deal with end effects

End effects are problematic for IAMs as they can distort optimal investment guidance, hence policy recommendations. Although the optimization horizon in Fig. 1 is relatively long, shorter horizons (e.g., 10–20 years, as used in myopic models) would exacerbate the impact of these terminal effects. This section reviews various approaches from the literature to mitigate end effects.

Horizon extension approach

A straightforward method to mitigate end effects is to extend the optimization horizon by an additional time period, ΔT_{add}, effectively pushing end effects beyond the window

of interest. The optimization problem remains as in (2.6)-(2.10), but the time set is extended to $[0, \ldots, T, \ldots, T + \Delta T_{add}]$. This approach is employed in the IAMs DICE (Nordhaus, 1992b) and REMIND (Luderer et al., 2015). For example, the REMIND model evaluates scenarios up to 2100, but the optimization horizon is extended by $\Delta T_{add} = 50$ years to 2150. Fig. 2 illustrates this approach.

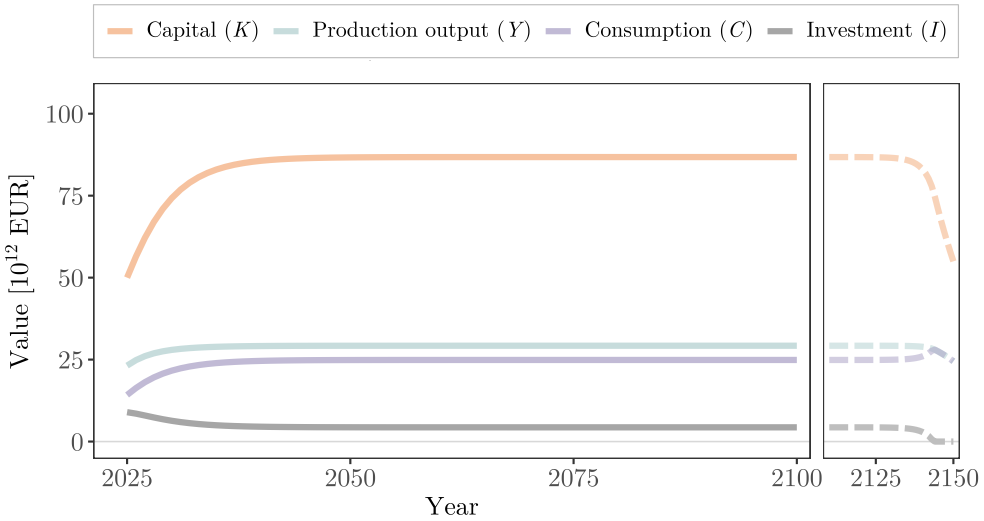


Fig. 2: | **Evolution of variables K, Y, C, and I in a Ramsey model formulated as finite-horizon nonlinear optimization problem with an extended optimization horizon.** We set the initial year ($t = 0$) to 2025, and the end year ($t = T$) is extended to 2150. This postpones end effects beyond the window of interest (2025 - 2100).

This approach is simple and effective but has limitations. It requires additional time steps, which increases computational complexity, and relies on input data far into the future, introducing uncertainties that can influence results within the window of interest. Furthermore, it is only applicable to models with long foresight and not to myopic (short-sighted) models, which deliberately use a short optimization horizon (e.g., 10–20 years) to more accurately reflect the behavior of real-world decision-makers.

End value approach

Another method to address end effects, without the shortcomings described above, is to include an end value U_{end} in the objective function. The objective of this approach is to ensure that the solution to the finite-horizon problem coincides with that of the infinite-horizon problem for all time steps $t \in \{0, \dots, T\}$:

$$\arg \max_{\{C_t\}_{t=0}^{\infty}} \sum_{t=0}^{\infty} U(C_t) e^{-\theta t} \Bigg|_{t \leq T} = \arg \max_{\{C_t\}_{t=0}^{T}} \left(\sum_{t=0}^{T} U(C_t) e^{-\theta t} + U_{end} \right). \tag{2.12}$$

The core idea is to account for the remaining capital stock K_{T+1} in the utility function, ensuring the finite-horizon optimization properly reflects the infinite-horizon trajectory. To the best of our knowledge, Barr and Manne (1967) were the first to propose an end value formulation for a Ramsey growth model:

$$U_{end} = \sum_{t=T+1}^{\infty} U(C^*_{T+1}\, e^{g(t-T)}) e^{-\theta t}. \tag{2.13}$$

Here, U_{end} represents the integrated tail of utility flows beyond the optimization horizon, effectively capturing the future utility beyond time step T. This formulation assumes that the economy has reached a balanced growth path by the end of the horizon and continues to grow at a predetermined rate g[2] during the infinite interval following T. Consequently, C^*_{T+1} is not a free decision variable; it denotes the consumption in time step $T+1$ dictated by the balanced growth path. Its value is determined by the capital stock K_{T+1} inherited from the end of the optimization horizon and must therefore be expressed as a function of K_{T+1}. The full derivation of U_{end} is provided in Appendix A. Applying this derivation, the end value can be written in closed form as given by eq. (A7):

$$U_{end} = \frac{e^{-\theta(T+1)}}{1 - e^{-\theta}} \ln(Y_{T+1} - K_{T+1}(e^g - 1 + \delta)).$$

Fig. 3 shows the results of solving the Ramsey problem with an end value added to the objective function. The economy converges to a steady state and no end effects occur. Herein, we assume no growth, so $g = 0$. However, the end value formulation in eq. (A7) is also valid for a growing economy ($g > 0$).

[2] The growth rate g is implied by model specification. In the simple case where growing labor is the only source of growth, it follows that $g = n$. Further details on growth dynamics are provided in Appendix G.

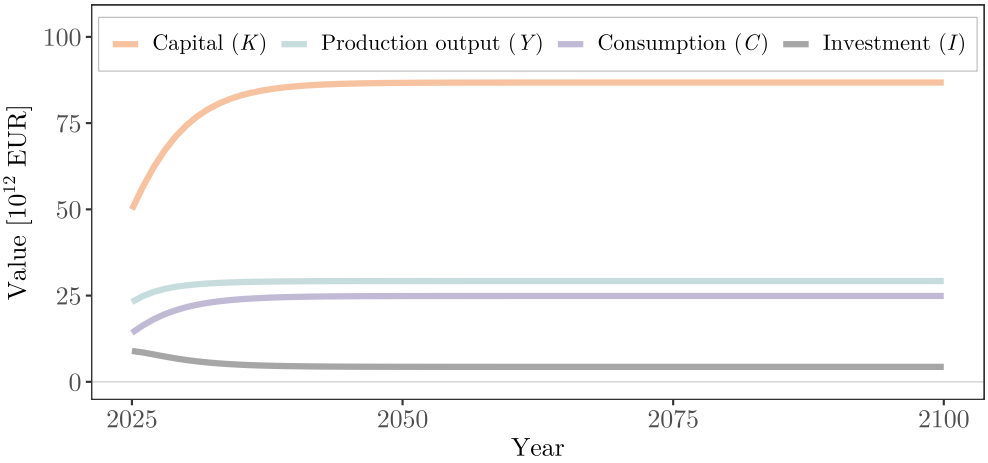


Fig. 3: | **Evolution of variables K, Y, C, and I in a Ramsey model formulated as finite-horizon nonlinear optimization problem with end value added to objective function**. We set initial year ($t = 0$) to 2025 and the end year ($t = T$) to 2100. We consider a non-growing economy ($n = 0$ and $A_t = A$, implying $g = 0$).

2.4 Related literature

The problem of end effects has been addressed from various perspectives in the literature, with different approaches proposed to mitigate their impact. Early theoretical work on approximating infinite-horizon problems with finite-horizon problems includes studies by Grinold (1977) and Flåm and J-B. (1987).

Lopes et al. (2015) focus on end value formulations, similar to the approach of Barr and Manne (1967), and provide formal proofs demonstrating that the finite-horizon problem with an end value can be equivalent to the infinite-horizon problem. They present formulations for the Ramsey and Uzawa-Lucas growth models and further test the end-value approach for economies experiencing shocks.

Another widely-used approach is state variable targeting, proposed by Lau et al. (2002). However, this method has been developed for models formulated as mixed complementarity problems rather than primal nonlinear optimization problems. The approach involves adding the constraint $I_T/I_{T-1} = Y_T/Y_{T-1}$ when solving the model. For this method to be used in a nonlinear optimization problem, an iterative solution would be required. It is also important to note that there are other mathematical techniques for solving infinite-horizon problems, aside from approximating them with finite-horizon formulations. For instance, Kelly and Kolstad (2001) present an algorithm for infinite-horizon integrated assessment models (IAMs), which relies on a neural network approximation of the value function within an iterative version of the Bellman equation.

The problem of end effects has also been explored extensively within the field of energy system modeling (Krishnan and McCalley, 2017). Various frameworks—such as GENeSYS-MOD (Löffler et al., 2017), LIMES (Osorio et al., 2023), NetPlan

(Krishnan et al., 2012), and Balmorel (Wiese et al., 2018)—utilize a salvage value to mitigate these effects. However, since these models function as cost-minimization problems, addressing end effects is often more intuitive: it typically suffices to subtract the value of the standing capital at the end of the horizon from the objective function. This approach aligns with standard accounting practices, such as how firms calculate terminal values on a balance sheet.

3 Methods

To our knowledge, no study has yet formulated an end value specifically for a hybrid model. Such a formulation could, for instance, be applied to detailed-process IAMs like DICE (Nordhaus, 1992b), MERGE (Manne et al., 1995), WITCH (Bosetti et al., 2007), or REMIND (Luderer et al., 2015). In this section, we first present the hybrid model used in this work: a Ramsey growth model coupled with a simplified energy system model, formulated as a nonlinear optimization program in primal form. Second, we describe two end value approaches: an explicit formulation, $U_{end}^{(1)}$, using an integrated tail, extending the method discussed in Section 2.3 (Approach 1), and an iterative formulation, $U_{end}^{(2)}$, based on shadow prices (Approach 2). Finally, we summarize the various foresight and end value approaches presented in this study and provide an intuitive interpretation of the type of real-world actor each corresponds to.

3.1 Hybrid model: Ramsey growth core coupled with an energy system model

The Ramsey growth component of the hybrid model is given by equations (3.1)–(3.5). While it follows the classical Ramsey growth formulation presented in Section 2.1, it is extended with additional variables representing the energy system. In particular, E_t denotes the useful energy generated in time step t, which, together with K_t and L_t, contributes to the CES production function. Investments in the energy sector are represented by $I_{E,t}$, while $I_{K,t}$ now denotes capital investments (previously I_t).

$$\max_{\{C_t\}} \quad \sum_{t=0}^{\infty} U(C_t) e^{-\theta t} \tag{3.1}$$

$$\text{s.t.} \quad Y_t = C_t + I_{K,t} + \boldsymbol{I_{E,t}} \tag{3.2}$$

$$\forall t \in \{0, \dots T\} \quad Y_t = A_t \left[\xi_K (\mu_K K_t)^\rho + \xi_L (\mu_L L_t)^\rho + \boldsymbol{\xi_E (\mu_E E_t)^\rho}\right]^{\frac{1}{\rho}} \tag{3.3}$$

$$L_t = L_0 e^{nt} \tag{3.4}$$

$$K_{t+1} = K_t (1 - \delta) + I_{K,t} \tag{3.5}$$

$$I_{K,t}, I_{E,t} \geq 0 \tag{3.6}$$

$$\text{with} \quad K_0 > 0 \quad \text{and} \quad L_0 > 0 \quad \text{given.}$$

The growth model and the energy system model are coupled through the variables $I_{E,t}$ and E_t, defined as:

$$I_{E,t} = cost_t = cost_t^{inv} + cost_t^{fuel} + cost_t^{OM} \tag{3.7}$$

$$E_t = prodSE_t. \tag{3.8}$$

Here, $I_{E,t}$ represents the total costs of the energy system in time step t, composed of investment ($cost_t^{inv}$), fuel ($cost_t^{fuel}$), and operation and maintenance ($cost_t^{OM}$) costs of the energy technologies. E_t, the useful energy, corresponds to the secondary energy $prod_t^{SE}$ generated by the energy technologies in time step t. A full description of the energy system part of the hybrid model is provided in Appendix B .

3.2 Approach 1: Explicit end-value formulation using an integrated tail

The first end-value approach we present - the explicit formulation using an integrated tail - is based on the methodology described in Section 2.3. Our goal is to determine an $U_{end}^{(1)}$ such that

$$\arg \max_{\{C_t\}_{t=0}^{\infty}} \sum_{t=0}^{\infty} U(C_t)e^{-\theta t}\Big|_{t\leq T} = \arg \max_{\{C_t\}_{t=0}^{T}} \left(\sum_{t=0}^{T} U(C_t)e^{-\theta t} + U_{end}^{(1)} \right). \tag{3.9}$$

The hybrid model includes an additional stock variable beyond capital: the standing energy capacity at the end of the horizon. These capacities incur costs, but through the generation of secondary energy they also contribute to the production function and, consequently, to utility. Therefore, the end value for the hybrid model $U_{end}^{(1)}$ must depend not only on the capital stock at the end of the horizon but also on the standing energy capacities.

The derivation starts from the same point as for U_{end}. We begin again with equation (2.13):

$$U_{end}^{(1)} = \sum_{t=T+1}^{\infty} U(C_{T+1}^{*}\, e^{g(t-T)})e^{-\theta t}.$$

The same assumptions as described in Section 2.3 apply. Recall that C_{T+1}^{*} is not a free decision variable; it denotes the consumption in time step $T+1$ dictated by the balanced growth path. We aim to express it in terms of the stock variables - here the remaining capital and energy capacities in time step T. The full derivation of $U_{end}^{(1)}$ is provided in Appendix C and the resulting end value expression in eq. (C15):

$$U_{end}^{(1)} = \frac{e^{-\theta(T+1)}}{1-e^{-\theta}} \ln\big(Y_{T+1} - I_{K,T+1}^{*} - I_{E,T+1}^{*}\big)$$

with
$$\begin{aligned} Y_{T+1} &= f(K_{T+1}, L_{T+1}, E_{T+1}) = f(K_{T+1}, L_{T+1}, \sum_{te} capacity_{T+1,te}\, \nu_{te}) \\ I_{K,T+1}^{*} &= K_{T+1}(e^{g} - 1 + \delta), \\ I_{E,T+1}^{*} &= \sum_{te} capacity_{T+1,te}\Big(\frac{p_{T+1,te}^{inv}}{\sum_{\tilde{t}=1}^{lifetime_{te}} e^{-g\tilde{t}}\omega_{\tilde{t}}} + p_{T+1,te}^{OM} + \frac{\nu_{te}}{\eta_{te}} p_{T+1,te}^{fuel}\Big) \end{aligned}$$

Here, $capacity_{T+1,te}$ denotes the total capacity of technology te in time step $T+1$; ν_{te} and η_{te} represent the capacity factor and conversion efficiency of technology te, respectively; $\omega_{\tilde{t}}$ is the depreciation parameter; and $p_{T+1,te}^{inv}$, $p_{T+1,te}^{OM}$, and $p_{T+1,te}^{fuel}$ correspond to the investment, operation and maintenance, and fuel costs of technology te in time step $T+1$.

3.3 Approach 2: Iterative end value formulation using shadow prices

The second end-value formulation we introduce moves away from the explicit integrated tail; instead, it utilizes a shadow price to provide a marginal proxy for all future utility flows. The optimization problem can be written as

$$\max_{\{C_t\}} \quad \sum_{t=0}^{T} U(C_t) e^{-\theta t} + U_{end}^{(2)} \tag{3.10}$$

$$\text{s.t.} \quad Y_t = C_t + I_{K,t} + I_{E,t} \tag{3.11}$$

$$\forall t \in \{0,\dots,T\} \quad Y_t = A_t \left[\xi_K(\mu_K K_t)^{\rho} + \xi_L(\mu_L L_t)^{\rho} + \xi_E(\mu_E E_t)^{\rho}\right]^{\frac{1}{\rho}} \tag{3.12}$$

$$L_t = L_0 e^{nt} \tag{3.13}$$

$$K_{t+1} = K_t(1-\delta) + I_{K,t} \tag{3.14}$$

$$U_{end}^{(2)} = (K_{T+1} + V_{capacity,T+1})\bar{\lambda}_{K,T+1} \tag{3.15}$$

$$I_{K,t}, I_{E,t} \geq 0 \tag{3.16}$$

$$\text{with } K_0 > 0 \text{ and } L_0 > 0 \text{ given.}$$

In this formulation, K_{T+1} denotes the remaining capital and $V_{capacity,T+1}$ the salvage value of the standing energy capacity at the end of the optimization horizon, given by eq. (B10). The term $\bar{\lambda}_{T,K+1}$ is treated as a parameter. Setting it equal to the shadow price that arises in the corresponding infinite-horizon problem, i.e.,

$$\bar{\lambda}_{K,T+1} = \lambda^{\infty}_{K,T+1},$$

ensures that the finite-horizon problem reproduces the infinite-horizon solution for time steps $t \in \{0, \dots, T\}$. The terminal shadow price $\bar{\lambda}_{K,T+1}$ then exactly captures the future utility and production potential embodied in these stocks. The mathematical background of this insight is provided in Appendix D, where we formulate the Lagrangian and the resulting KKT conditions of the Ramsey growth model. We show that setting $\bar{\lambda}_{K,T+1} = \lambda^{\infty}_{K,T+1}$ ensures that the solution to the finite-horizon problem coincides with the infinite-horizon solution over the interval $t \in \{0, \dots, T\}$. Furthermore, using the previously derived KKT conditions, we identify the implicit terminal shadow price imposed by the integrated tail approach described in Sections 2.3 and 3.2.

In practice, when solving hybrid models numerically, $\lambda^{\infty}_{K,T+1}$ is generally unknown. Hence, we employ an iterative approach: the finite-horizon problem is solved repeatedly, with the terminal shadow price being updated at each iteration i. We denote the end value in iteration i as:

$$U^{(2)}_{\text{end}|i} = (K_{T+1}, V_{capacity,T+1})\lambda_{K,T+1|i}. \tag{3.17}$$

The iterative process begins at $i = 0$ with no end value imposed:

$$\lambda_{K,T+1|i=0} = 0. \tag{3.18}$$

Although more sophisticated initial estimates could be employed to improve convergence speed in practical applications, the focus of this study is on the existence and robustness of convergence rather than computational efficiency. We therefore use the simplest initialization and set the initial terminal shadow price equal to zero.

For subsequent iterations, we define an update mapping $\mathcal{T}$ that specifies how the shadow price at time step $T + 1$ is determined from the shadow price at time step T.

$$\lambda_{K,T+1|i+1} = \mathcal{T}(\lambda_{K,T|i}). \tag{3.19}$$

The algorithm can be summarized as follows:

Initialize: $\lambda_{K,T+1|i=0} = 0$

Iteration: $i = 0$

Repeat until convergence:

1: Solve $\max_{\{C_t\}} \sum_{t=0}^{T} U(C_t)e^{-\theta t} + (K_{T+1}, V_{capacity,T+1})\lambda_{K,T+1|i}$ **s.t.** (3.11) – (3.14)

2: Update $\lambda_{K,T+1|i+1} = \mathcal{T}(\lambda_{K,T|i})$

3: Check convergence:

If $\left|\frac{\lambda_{K,T+1|i+1} - \lambda_{K,T+1|i}}{\lambda_{K,T+1|i}}\right| < \epsilon$, **set** $\bar{\lambda}_{K,T+1} = \lambda_{K,T+1|i}$ **and stop**

4: $i \leftarrow i + 1$

This work analyzes two iterative update mappings $\mathcal{T}$. Approach (I) assumes that the system has reached a balanced growth path at time step T, which implies all variables growing at rate g and shadow prices declining at rate $(\theta + g)$:

$$\lambda_{K,T+1|i+1} = \mathcal{T}_I(\lambda_{K,T|i}) = \lambda_{K,T|i} \cdot e^{-(\theta+g)}. \tag{3.20}$$

Approach (II) assumes that the terminal shadow price develops proportionally to its recent change, effectively extrapolating the trend from the last two periods:

$$\lambda_{K,T+1|i+1} = \mathcal{T}_{II}(\lambda_{K,T|i}) = \lambda_{K,T|i} \cdot \frac{\lambda_{K,T|i}}{\lambda_{K,T-1|i}}. \tag{3.21}$$

While a formal analytical proof of convergence for these two approaches is beyond the scope of this study, we perform a rigorous numerical validation in Section 4 to evaluate their computational stability. Our results demonstrate that both approaches converge to a stable fixed point as the iteration count $i \to \infty$. Specifically, we show that for both update mappings, the terminal shadow price $\lambda_{K,T+1|i}$ converges to the infinite-horizon value $\lambda^{\infty}_{K,T+1}$ as both $T \to \infty$ and $i \to \infty$.

3.4 Overview of foresight assumptions and end value formulations

Previous sections introduced several approaches to modeling foresight and approximating an infinite-horizon with a finite one. Table 1 summarizes these approaches and provides an intuitive interpretation of the type of social planner each one represents. Their numerical implementation is discussed in Section 4.1.

Table 1: Foresight assumptions and end value formulations

Foresight	**Handling of time horizon**	**Actor**	**Intuitive description**
(1) Perfect $t \in \{0, 1, 2, \dots\}$		*The Clairvoyant*	"I have the gift to look into eternity and optimize accordingly."
(2) Myopic $t \in \{0, \dots, T\}$	No end value	*The Apocalyptist*	"I assume the world ends after time step T, so remaining capital has no value beyond the horizon."
(3) Myopic $t \in \{0, \dots, T + \Delta T_{add}\}$	Extended horizon	*The Lazy Myope*	"I don't want to think too much about end values and simply extend the horizon by a few periods."
(4) Myopic $t \in \{0, \dots, T\}$	Approach 1 (integrated tail): End value $U^{(1)}_{\text{end}}$	*The Pensioner*	"I assume the world freezes after time T and I want to live indefinitely off the returns generated by my accumulated capital."
(5) Myopic $t \in \{0, \dots, T\}$	Approach 2 (shadow prices): End value $U^{(2)}_{\text{end}}$ $\bar{\lambda}_{K,T+1} = \lambda^{\infty}_{K,T+1}$	*The Clairvoyant's Friend*	"I optimize only until time T but my friend the Clairvoyant tells me the exact shadow value of capital beyond my horizon."
(6) Myopic $t \in \{0, \dots, T\}$	Approach 2 (shadow prices): End value $U^{(2)}_{\text{end}}$ $\bar{\lambda}_{K,T+1}$ iteratively with $\mathcal{T}_I$	*The Overambitious Iterator*	"I want the economy to reach its balanced growth path already at time T and keep iterating until I find a terminal shadow price that enforces this."
(7) Myopic $t \in \{0, \dots, T\}$	Approach 2 (shadow prices): End value $U^{(2)}_{\text{end}}$ $\bar{\lambda}_{K,T+1}$ iteratively with $\mathcal{T}_{II}$	*The Trend Analyzing Iterator*	"I want the economy to develop in a consistent way, so I keep iterating until the trend after time T matches the trend at the end of the horizon."

4 Results

This section first presents the experimental setup and the numerical implementation of all scenarios. It then compares the performance of the two end value methods considered, first for a pure Ramsey growth model and subsequently for the hybrid model.

4.1 Experimental setup

For an exhaustive assessment of the various end value assumptions, all approaches shown in Table 1 are formulated as optimization problems and solved numerically. However, regarding perfect foresight, we do not compute a solution for the true infinite-horizon problem. Instead, we use a sufficiently long optimization window to serve as a numerical approximation of the perfect foresight assumption. Specifically, we set $t = T_{PF}$ to 2150; this ensures that all end effects occur beyond the period of interest, as results are assessed only until 2080. For myopic foresight, we consider two degrees of myopia: a strong version with an optimization window ending in 2030, and a moderate version with the optimization window ending in 2080.

Table 2 summarizes the foresight approaches, their corresponding objective functions, and the scenario acronyms used in the comparison. Additional details on the model parametrization are provided in Appendix E. Since perfect foresight is implemented numerically by extending the optimization horizon to 2150, the perfect foresight scenarios (1) are equivalent to the myopic extended-horizon scenarios (3). Scenarios (5) represent a purely theoretical benchmark in which the terminal shadow prices are taken directly from the corresponding perfect foresight solution. By construction, this formulation reproduces the exact perfect foresight solution regardless of the horizon length or the presence of oscillations. We include this benchmark primarily to validate the terminal-value formulation; because it relies on information from a perfect foresight run, it does not represent a genuinely myopic decision-maker.

The optimization models have been implemented in GAMS (GAMS Development Corporation, 2025) as D-NLP problems and solved using the CONOPT solver. The source code for all models and experiments is publicly accessible on Zenodo (https://doi.org/10.5281/zenodo.21496140).

Table 2: Numerical implementation of the different foresight approaches. In all scenarios $t = 0$ is set to 2025, $t = T_{PF}$ to 2150, $t = T_{MF}$ to either 2030, 2080 or 2100, and $\Delta T_{add} = 50$. The column *Scenarios* lists the acronyms for the case studies considered, where 'R' denotes the simple Ramsey growth model and 'H' denotes the hybrid model.

Foresight		**Objective function**	**Scenarios**
(1) Perfect (PF)		$\sum_{t=0}^{T_{PF}} U(C_t) \cdot e^{-\theta t}$	*R-PF* *H-PF*
(2) Myopic (MF)	No end value	$\sum_{t=0}^{T_{MF}} U(C_t) \cdot e^{-\theta t}$	*R-MF-2030*, *R-MF-2080* *H-MF-2030, H-MF-2080*
(3) Myopic	Extended horizon	$\sum_{t=0}^{T_{MF}+\Delta T_{add}} U(C_t) \cdot e^{-\theta t}$	*R-PF* *H-PF*
(4) Myopic	Approach 1 (integrated tail): End value $U_{\text{end}}^{(1)}$	$\sum_{t=0}^{T_{MF}} U(C_t) \cdot e^{-\theta t} + U_{end}^{(1)}$	*R-MF-2030-Uend1* *R-MF-2080-Uend1* *H-MF-2030-Uend1* *H-MF-2080-Uend1*
(5) Myopic	Approach 2 (shadow prices): End value $U_{\text{end}}^{(2)}$ $\bar{\lambda}_{K,T+1} = \lambda_{K,T+1}^{\infty}$	$\sum_{t=0}^{T_{MF}} U(C_t) \cdot e^{-\theta t} + U_{end}^{(2)}$	*R-MF-2030-Uend2-PF* *R-MF-2080-Uend2-PF* *H-MF-2030-Uend2-PF* *H-MF-2080-Uend2-PF*
(6) Myopic	Approach 2 (shadow prices): End value $U_{\text{end}}^{(2)}$ $\bar{\lambda}_{K,T+1}$ iteratively with $\mathcal{T}_I$		*R-MF-2030-Uend2-I* *R-MF-2080-Uend2-I* *H-MF-2030-Uend2-I* *H-MF-2080-Uend2-I*
(7) Myopic	Approach 2 (shadow prices): End value $U_{\text{end}}^{(2)}$ $\bar{\lambda}_{K,T+1}$ iteratively with $\mathcal{T}_{II}$		*R-MF-2030-Uend2-II* *R-MF-2080-Uend2-II* *H-MF-2030-Uend2-II* *H-MF-2080-Uend2-II*

4.2 Ramsey growth model

This section analyzes the performance of the two end-value methods within a simple Ramsey growth model (as defined in equations (2.6)–(2.11)). To provide a benchmark for comparison, we first present the perfect foresight scenario. This serves as the reference point against which the performance of the end-value methods is evaluated throughout this section.

Figure 4 shows the solution of the Ramsey growth model with no end value, for a horizon extending to 2150 - a scenario we refer to as perfect foresight. The trajectory is analogous to Fig. 1, characterized by a transition phase, a steady-state phase, and a final phase dominated by end .

Panel (a) displays the primal variables — capital, output, consumption, and investment — whose trajectories are analogous to Fig. 1, characterised by a transition phase, a steady-state phase, and a final phase dominated by end effects. Panel (b) shows the associated real interest rate, obtained from the shadow price of capital. At the transition phase it exceeds the pure rate of time preference θ because consumption is still growing, and converges to $r = r^* = \theta$ once the steady state is reached. Since the system reaches its steady state[3] before 2080, these results - for the period until 2080 - serve as a substitute for the true infinite-horizon solution.

To evaluate the methods' performance across different system dynamics, we consider two boundary settings: one in which the horizon ends while the system is still in transition ($T = 2030 < T^*$), and another in which the horizon is long enough for the system to have reached its steady state ($T = 2080 > T^*$). The 2030 horizon constitutes an extreme case, as in realistic IAM settings the system is unlikely to be as far from equilibrium as it is here. This choice is deliberate, as it makes the resulting effects easier to identify. In practical settings, however, these effects might be smoother and less pronounced.

[3] We define the steady state as the first period t^* such that the capital growth rate remains below a threshold $\varepsilon = 10^{-4} + e^g - 1$ for ten consecutive periods:

$$\frac{k_{t+1-i} - k_{t-i}}{k_{t-i}} < \varepsilon \quad \forall i = 0, \ldots, 9.$$

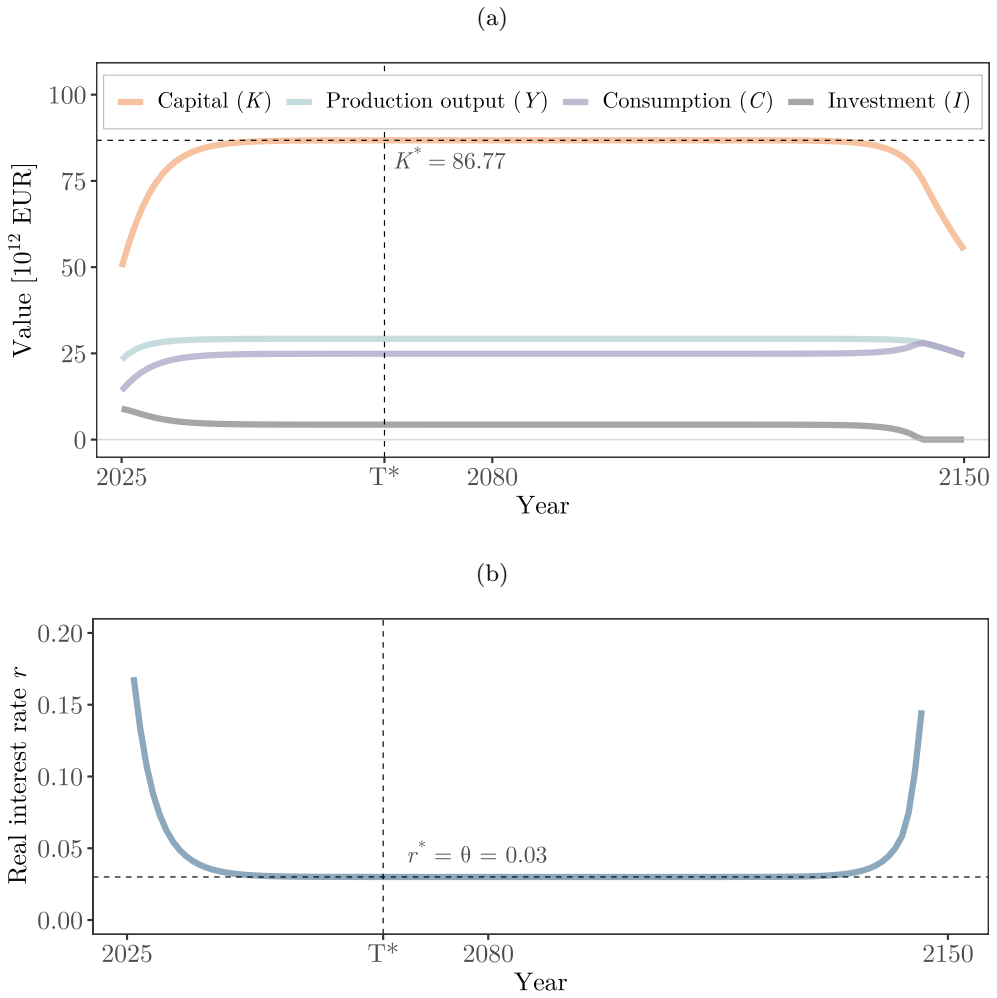
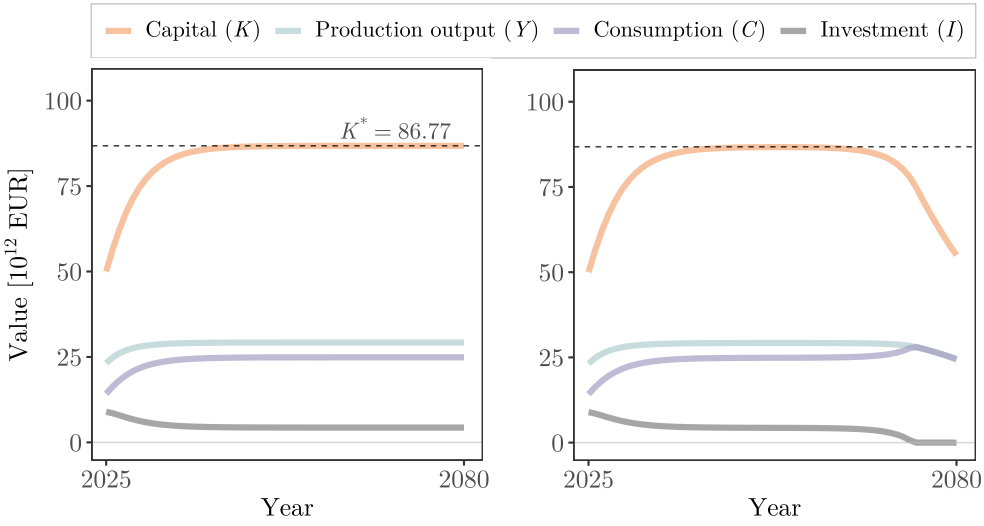


Fig. 4: Ramsey growth model under perfect foresight (scenario *R-PF*, as defined in Table 2). (a) Primal variables K, Y, C, I_K. (b) Real interest rate $r_t = \ln(\lambda_{K,t}/\lambda_{K,t+1})$. The initial year $t = 0$ is set to 2025 and the end year ($t = T$) to 2150. We consider a non-growing economy ($n = 0$ and $A_t = A$, implying $g = 0$). K^* denotes the value of capital at steady state, and $T^* = 2064$ the year when steady state is reached. At steady state, $r^* = \theta$, the pure rate of time preference.

Foresight until 2080: $T > T^*$

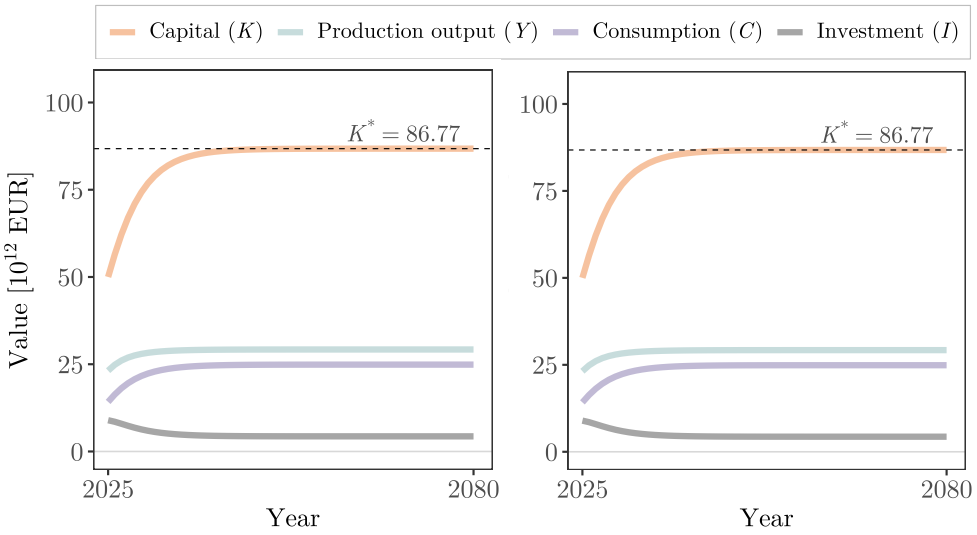
Figure 5a presents the perfect foresight scenario (*R-PF*) and Fig. 5b the myopic foresight case with a horizon ending in 2080 (*R-MF-2080*). In the *R-PF* scenario all variables presented—K, Y, C, and I—reach their steady-state values and remain constant throughout the displayed time window. By contrast, the *R-MF-2080* scenario exhibits pronounced end effects. As the end of the finite horizon approaches, the model no longer perceives benefits from investment and instead consumes a large share of the accumulated capital. The objective of the end-value approaches is to minimize these terminal distortions and effectively guide the myopic *R-MF-2080* solution toward the perfect foresight *R-PF* outcome.



(a) Scenario *R-PF* (b) Scenario *R-MF-2080*

Fig. 5: **Evolution of variables K, Y, C, and I in the Ramsey growth model under perfect and myopic foresight (scenarios *R-PF* and *R-MF-2080*, as defined in Table 2)**. The initial year ($t = 0$) is set to 2025. K^* denotes the value of capital at steady state.

Figure 6a presents the results for perfect foresight up to 2080, corresponding to the infinite-horizon solution, while Fig. 6b displays the results for the myopic foresight case with an end value applied. As the trajectories are identical across all end value approaches, only a single representative plot is shown. The comparison demonstrates that the end value approaches approximate the infinite-horizon solution with high accuracy. This conclusion is supported both visually and numerically: absolute differences across scenarios remain below 2×10^{-5} for all variables, which is negligible in the context of a numerical experiment. Relative differences for the variables K and I_K are reported in Tables F1 and F2.



(a) Scenario *R-PF*

(b) Scenarios *R-MF-2080-Uend1, R-MF-2080-Uend2-PF, R-MF-2080-Uend2-I, R-MF-2080-Uend2-II*

Fig. 6: **Evolution of variables K, Y, C, and I in the Ramsey growth model under (a) perfect foresight and (b) myopic foresight with an end value added to the objective function**. Scenarios are defined in Table 2. All end value formulations in panel (b) yield the same result. The initial year ($t = 0$) is set to 2025. K^* denotes the value of capital at steady state.

While all end value approaches yield the same final results, the iterative approaches exhibit distinct convergence behaviors. Figure 7 illustrates the convergence paths for mappings τ_I and τ_{II}. Relative errors per iteration are reported in Appendix Tables F3 and F4. These results indicate that the end value using mapping τ_I converges significantly faster than that with τ_{II}. Consequently, the choice of mapping can have a substantial impact on computational time.

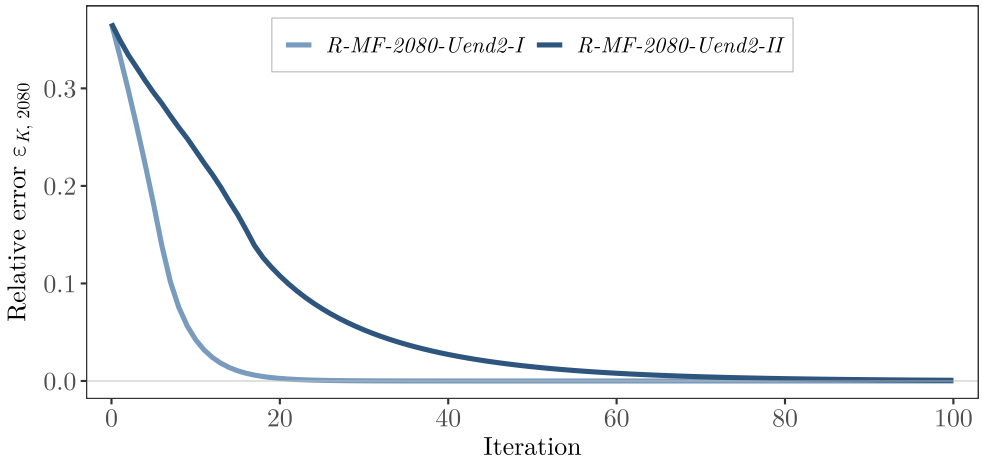
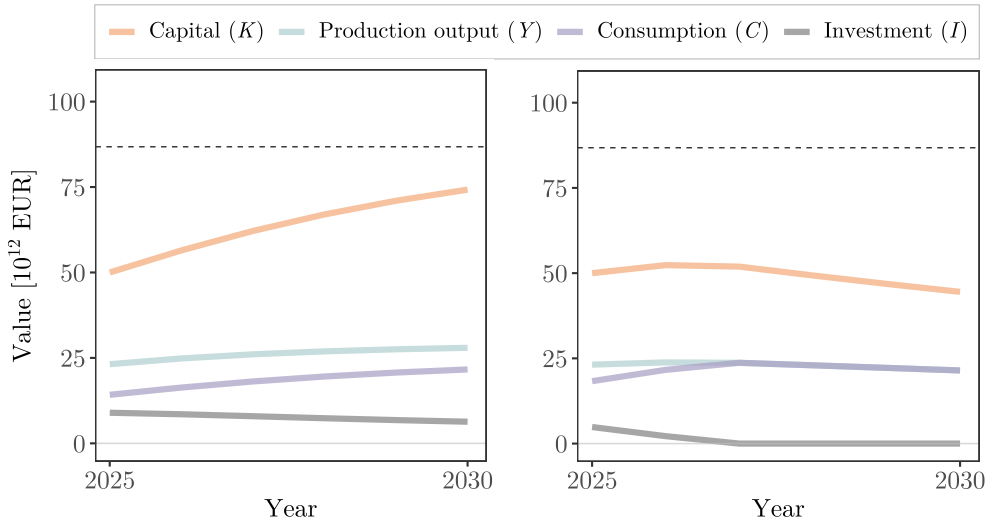


Fig. 7: **Convergence behavior of iterative approaches in Ramsey growth model with myopic foresight until 2080.** Shown is the evolution of the relative error $\epsilon_{K,2080} = \frac{K_{2080|PF} - K_{2080|i}}{K_{2080|PF}}$ over 100 iterations, comparing the performance of mapping τ_I (light blue) and τ_{II} (dark blue) — corresponding to scenarios *R-MF-2080-Uend2-I* and *R-MF-2080-Uend2-II* as defined in Table 2, respectively.

Foresight until 2030: $T < T^*$

Figure 8a presents the perfect foresight solution shown up to 2030, corresponding to the initial segment of an infinite-horizon problem, while Fig. 8b shows the myopic foresight solution in the absence of any end value. In the perfect foresight scenario (*R-PF*), the system is still in transition by 2030 and has not yet reached its steady state. Under myopic foresight (*R-MF-2030*), end effects fall entirely within the optimization horizon; specifically, investment drops to zero from 2027 onward, and the capital stock is subsequently drawn down.



(a) Scenario *R-PF* (b) Scenario *R-MF-2030*

Fig. 8: Evolution of variables K, Y, C, and I in the Ramsey growth model under perfect and myopic foresight (scenarios *R-PF* and *R-MF-2030*, as defined in Table 2). The initial year ($t = 0$) is set to 2025.

Figure 9 illustrates the trajectories for perfect foresight (*R-PF*), myopic foresight without an end value (*R-MF-2030*), and the various end-value approaches. In contrast to the $T = 2080$ case, where all end-value approaches yield identical solutions (see Fig. 7), a shorter horizon ($T = 2030$) leads to varying outcomes across the different end-value approaches.

The end value $U_{end}^{(1)}$ leads to substantially higher investment levels — for instance, investment in year 2030 is around 40% higher than in the perfect foresight benchmark. Consequently, this results in a higher capital stock K at the end of the horizon. This behavior aligns with the interpretation of a "pensioner" agent (see Table 1), who finds it optimal to sacrifice some consumption during the 2025–2030 period in order to increase utility over the post-2030 infinite horizon.

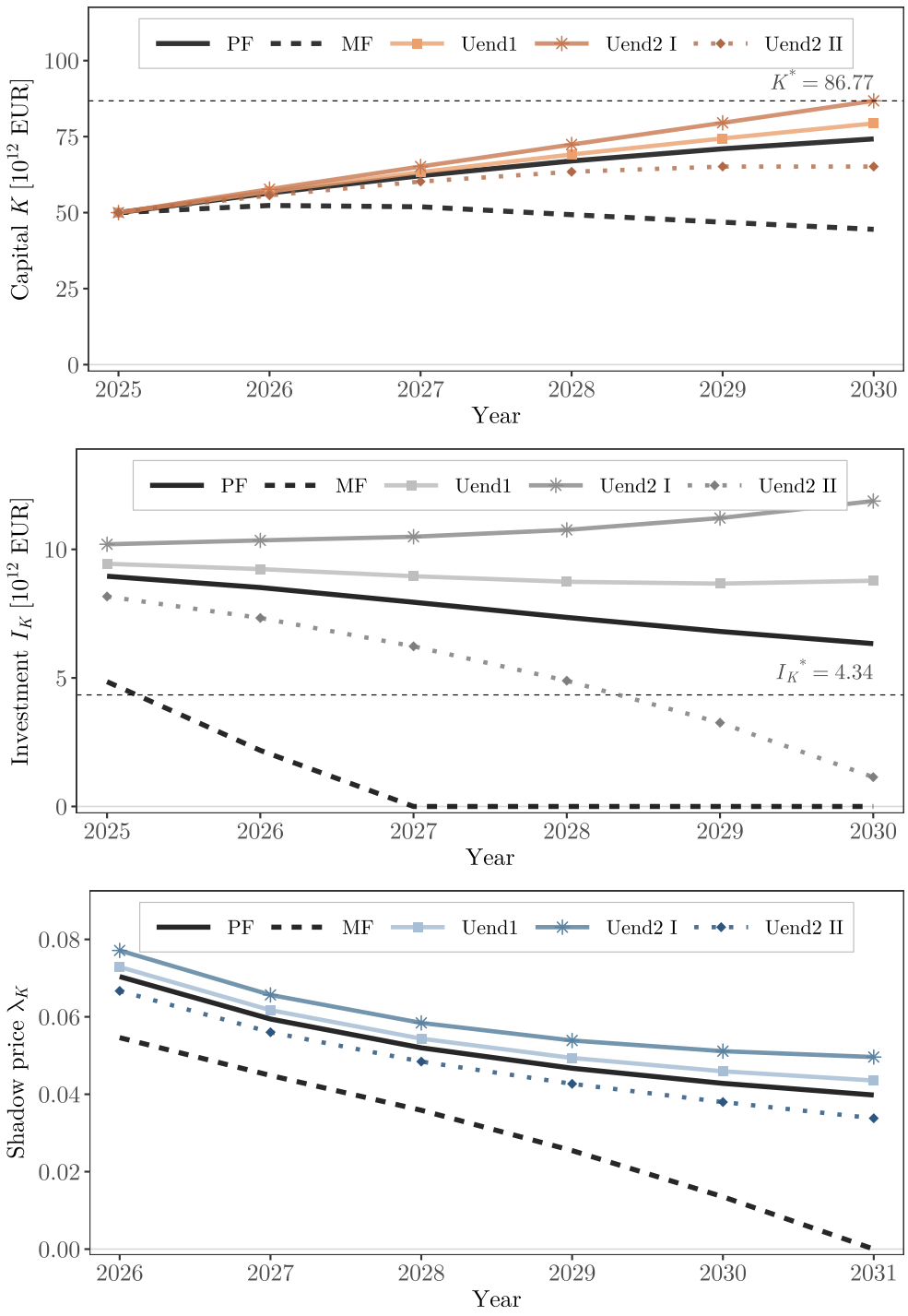


Fig. 9: **Evolution of capital K, investment I_K, and shadow price λ_K in the Ramsey growth model under perfect foresight, myopic foresight, and myopic foresight with an end value added to the objective function.** The scenarios shown are *R-PF*, *R-MF-2030*, *R-MF-2030-Uend1*, *R-MF-2030-Uend2-I*, and *R-MF-2030-Uend2-II*. Their definition is provided in Table 2. The initial year ($t = 0$) is set to 2025. K^* and I_K^* denote the value of capital and investments at steady state.

Using the end value $U^{(2)}_{end}$ with mapping τ_I leads to even higher investment levels — approximately 88% higher in 2030 compared to *R-PF* — such that capital reaches its steady-state value K^* already in 2030. This result is consistent with the definition of τ_I in Section 3.3, which assumes that shadow prices decline at rate $(\theta + g)$. Under this assumption, the mapping effectively forces the system onto the balanced growth path (or in the present case with $g = 0$, into the steady state).

By contrast, $U^{(2)}_{end}$ with mapping τ_{II} results in lower investment and capital levels than under perfect foresight. While mapping τ_I overestimates the shadow price $\bar{\lambda}_{K,T+1}$ by imposing balanced-growth dynamics, mapping τ_{II} underestimates the shadow price by extrapolating its value at $T + 1$ from shadow prices in T and $T - 1$.

Finally, it is important to note that scenario *R-MF-2030-Uend2-PF* produces exactly the same solution as the perfect-foresight scenario (*R-PF*) and is therefore not shown explicitly. This outcome is consistent with the theoretical considerations presented in Section 3.3.

4.3 Hybrid model

This section turns to the performance of the different end-value approaches in the hybrid model, as formulated in equations (3.1)–(3.8). The full model parametrization is provided in Appendix E.

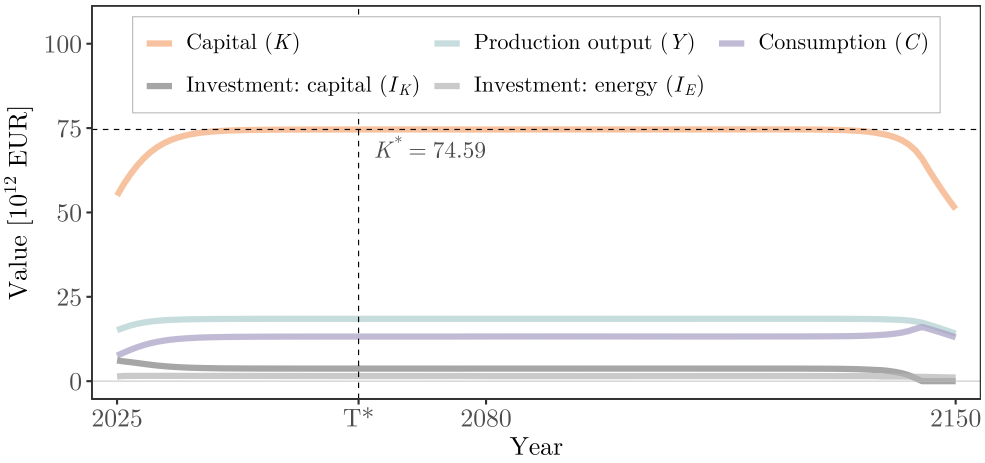
Once more, we begin by presenting the benchmark scenario. Figure 10 shows the evolution of macroeconomic system variables K, Y, C, I_K and I_E, while Figure 11 focuses on the evolution of the energy sector, depicting capacity additions and the total capacity stock – all under perfect foresight.

At first glance, the variables shown in Figure 10a exhibit dynamics similar to those of the simple Ramsey growth model. However, a closer analysis of capital K (Figure 10b), and investment into the energy system I_E (Figure 10c) reveals differences. Compared to the Ramsey model, the hybrid model converges more slowly to its steady state, which is also less stable. In particular, a discontinuity emerges around the year 2074. The latter can be attributed to the finite lifetime of technologies (50 years). While the depreciation rate follows a smooth trajectory over the lifetime of each technology, once the maximum lifetime is reached, the remaining value of the technology is set to zero and the capacity is fully retired. Finally, although the system reaches its steady state around 2060, it exhibits remaining oscillations thereafter, on the order of 0.1% for investment in capital K and 1% for investments into the energy system I_E.

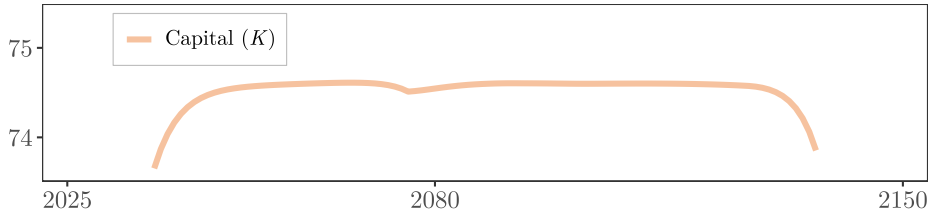
Figure 11 shows capacity additions and total installed capacity for coal and gas technologies. In this stylized model, which is used solely for demonstration purposes, we include only these two technologies. The energy-system representations of real IAMs are considerably more complex and realistic than the one used in this hybrid model; the simple setup adopted here was chosen for illustrative clarity and is sufficient to demonstrate the effects of the different end-value formulations. Coal and gas provide a useful contrast for analyzing dynamics across scenarios, as coal is characterized by higher investment costs but lower fuel costs, whereas gas features lower investment costs and higher fuel costs. Accordingly, the model invests predominantly in coal throughout most of the horizon, reflecting its lower long-term cost. Toward the end of

the horizon, however, when end effects become relevant, the model shifts investment toward gas, as technologies with lower upfront costs are preferred when the remaining planning horizon is short. Examining capacity additions reveals some remaining oscillations, even after the discontinuity around year 2075. These arise from the assumed polynomial depreciation profile. Under geometric depreciation, the capacity additions paths is smoother (see Figure F1). However, we deliberately chose to analyze polynomial depreciation here, as it is arguably more realistic and allows us to demonstrate that the end-value approaches performs well even under a more complex depreciation formulation.

(a) Evolution of variables



(b) Detailed view: Capital



(c) Detailed view: Energy investments

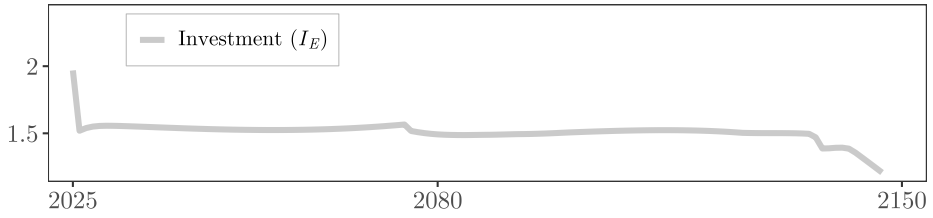


Fig. 10: **Evolution of variables K, Y, C, I_K, and I_E in the hybrid model under perfect foresight (scenario *H-PF*, as defined in Table 2)**. The initial year ($t = 0$) is set to 2025 and the end year ($t = T$) to 2150. We consider a non-growing economy ($n = 0$ and $A_t = A$, implying $g = 0$). K^* denotes the value of capital at steady state.

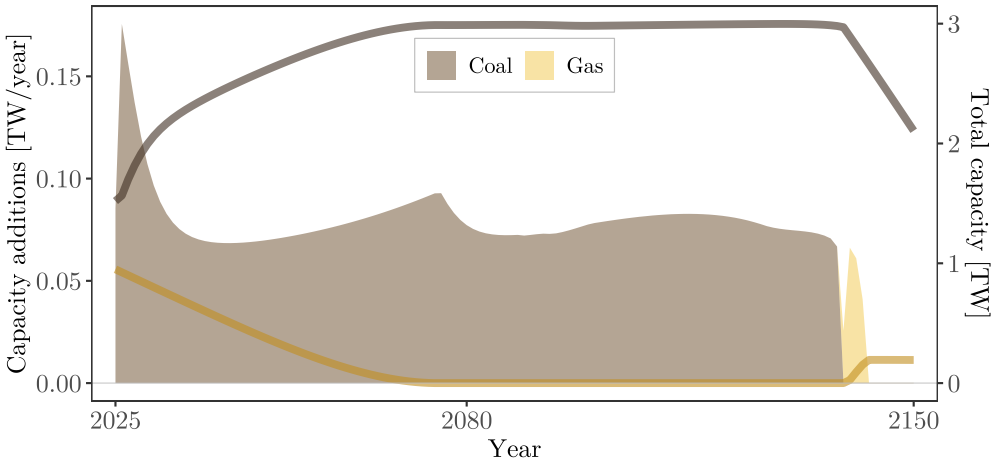


Fig. 11: **Capacity additions (shaded area) and total capacity (lines) of coal and gas under perfect foresight (scenario *H-PF*, as defined in Table 2).** The initial year ($t = 0$) is set to 2025 and the end year ($t = T$) to 2150. We consider a non-growing economy ($n = 0$ and $A_t = A$, implying $g = 0$).

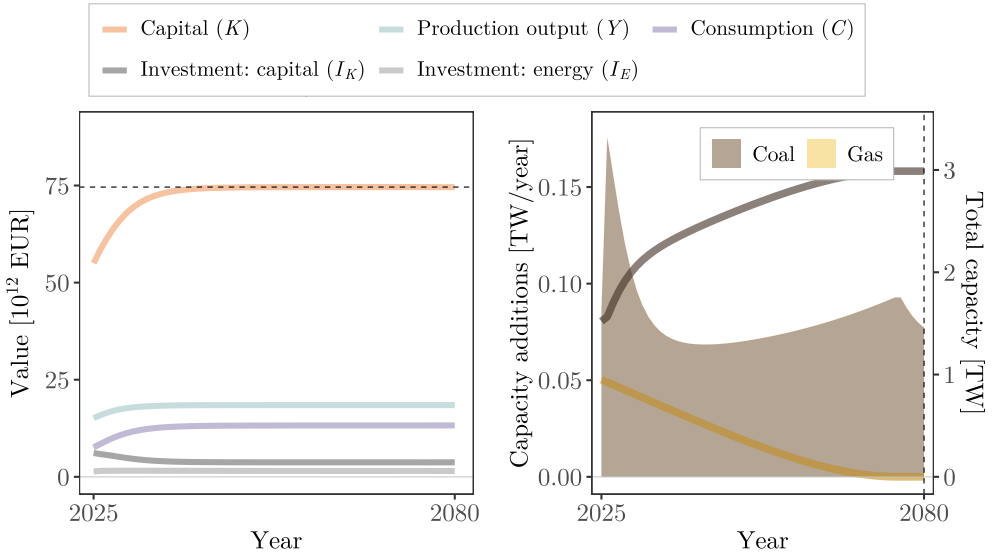
Foresight until 2080: $T > T^*$

Fig. 12 presents the results for perfect foresight (*H-PF*) up to the year 2080 in Fig. 12a and 12b, for myopic foresight in Fig. 12c and 12d, and for myopic foresight with an end value in Fig. 12e and 12f. The different end-value formulations approximate the perfect foresight trajectory to a comparable degree, with only minor differences between them; we therefore show only the results for the end value $U_{end}^{(2)}$ with mapping τ_{II} (scenario *H-MF-2080-Uend2-II*) as a representative scenario. The performance of the remaining end values is provided in Appendix Fig. F2.

When considering investments in generation technologies, one can see that under perfect foresight (Fig. 12b) the model invests solely in coal – the technology with lower levelized costs of electricity – while the total gas capacity gradually declines toward zero. Due to the assumed technology lifetime of 50 years, the energy-system component of the model requires substantially more time to converge to its steady state than the macroeconomic counterpart.

For myopic foresight, total investments decline toward zero at the end of the planning horizon (Fig. 12c), which mirrors the outcome of the Ramsey growth model. Regarding the technology mix (Fig. 12d), the model initially invests in coal, but shifts toward gas investments toward the end of the horizon. This transition is driven by the lower capital costs of gas relative to coal, which increasingly outweigh its higher fuel costs as the remaining planning horizon shortens.

For the scenario with an end value (shown here for *H-MF-2080-Uend2-II*, though the same insights apply to the other end-value scenarios), the approach reproduces the perfect foresight solution remarkably well. Notably, it captures both the discontinuity and oscillations present in the benchmark case. However, a closer examination reveals differences in the final time step (2080). These occur because, in the terminal period, the model no longer distinguishes between investments in capital and investments in the energy system, as both are treated equivalently beyond the horizon. While total investment and consumption levels remain correct, the allocation between capital investment and energy-sector investment is distorted. This effect emerges as both the capital accumulation equation and the capacity accumulation equations are formulated such that investments made in period T only affect aggregate capital or capacity in period $T + 1$. If investments in period T were instead affecting cumulative variables already in the same period, this distortion would not arise. Importantly, this limitation affects only the final time step and has no impact on earlier periods. Nevertheless, it should be noted that when implementing end values in a hybrid model, an additional time step is required to correct for this terminal effect.



(a) Scenario *H-PF* (b) Scenario *H-PF*

(c) Scenario *H-MF-2080* (d) Scenario *H-MF-2080*

(e) Scenario *H-MF-2080-Uend2-II* (f) *H-MF-2080-Uend2-II*

Fig. 12: **Evolution of variables K, Y, C, I, *capacityADD*, and *capacity* in the hybrid model under perfect and myopic foresight. The scenarios are defined in Table 2**. Capacity additions are shown as shaded areas, while total capacity is indicated by the lines. The initial year ($t = 0$) is set to 2025.

Tables 3 and 4 present the relative numerical errors for capital investment and coal capacity additions between the perfect foresight solution and the myopic solutions with different end-value formulations. For all end values, the relative differences – evaluated over the period 2075–2080, where end effects are most prominent – remain below 0.5%. However, very pronounced deviations emerge in the final time step (2080), further highlighting that end values in hybrid models lead to distortions in the terminal period.

Overall, the accuracy of end values in the hybrid model is slightly lower than in the Ramsey growth model. For comparison, the relative error $\epsilon_{I_K} = \frac{I_{K|\text{PF}} - I_K}{I_{K|\text{PF}}}$ for the Ramsey model is lower than 0.002 % for all scenarios, as reported in the Appendix in Table F2. This discrepancy between the results obtained with the Ramsey and hybrid model can likely be attributed to the remaining oscillations and the, consequently, less stable steady state in the hybrid model. Nevertheless, deviations from the perfect foresight solution of less than 0.5% are of little relevance from a practical perspective, especially when compared to the uncertainty inherent in empirical data and parameter calibration in real-world applications. We therefore conclude that all end values presented in this article perform robustly also in a hybrid model setting.

Table 3: Relative error $\epsilon_{I_K} = \frac{I_{K|PF} - I_K}{I_{K|PF}}$

	2075	2076	2077	2078	2079	2080
Uend1	0.08 %	0.1 %	0.2 %	0.3 %	0.4 %	0.4 %
Uend2 PF	0.01 %	0.01 %	0.01 %	0.01 %	0.01 %	**3 %**
Uend2 I	0.06 %	0.09 %	0.1 %	0.2 %	0.2 %	**63 %**
Uend2 II	0.03 %	0.04 %	0.05 %	0.06 %	0.07 %	**83 %**

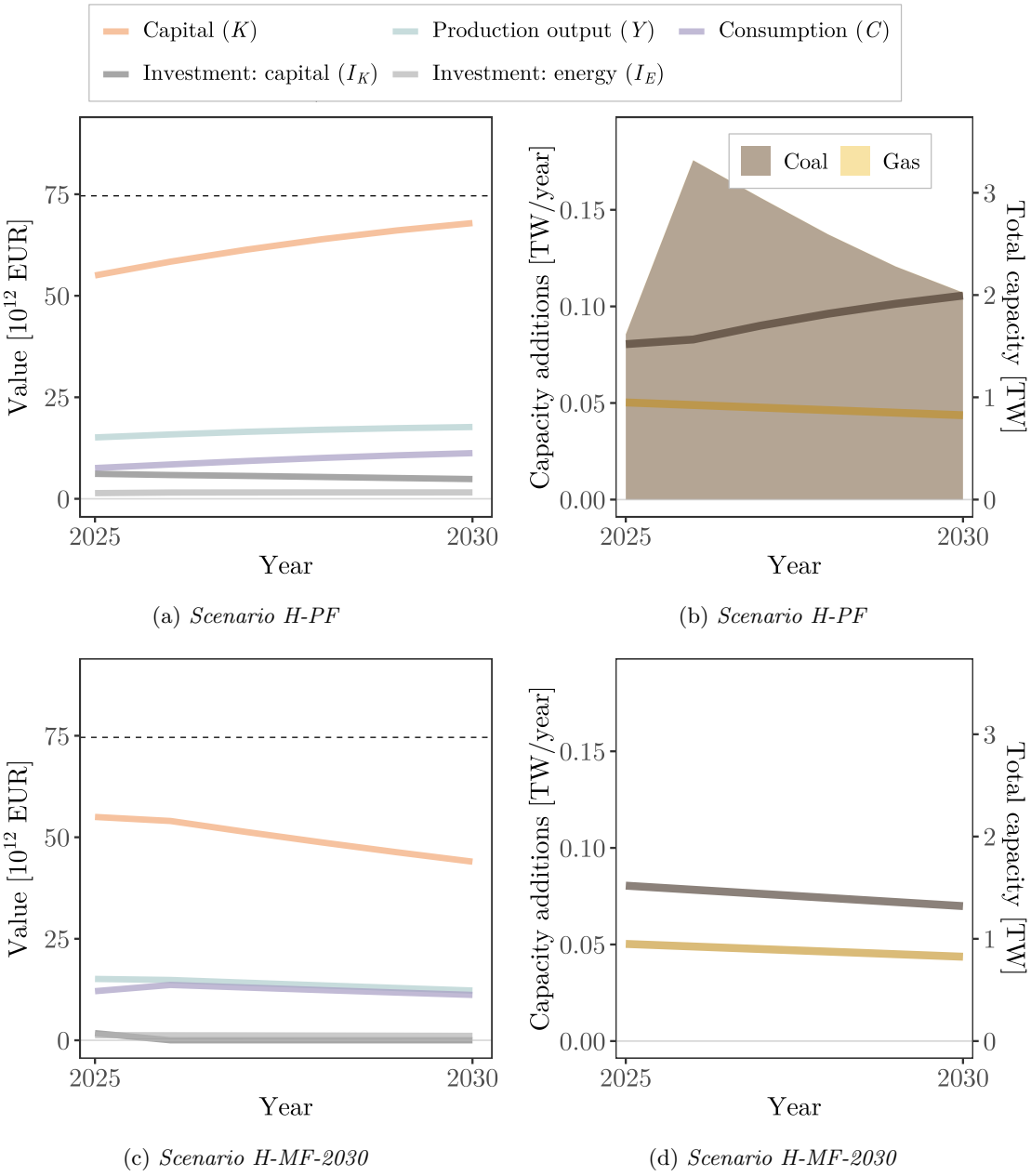
Table 4: Relative error $\epsilon_{capacityADD_{coal}} = \frac{capacityADD_{coal|PF} - capacityADD_{coal}}{capacityADD_{coal|PF}}$

	2075	2076	2077	2078	2079	2080
Uend1	0.01 %	0.02 %	0.03 %	0.04 %	0.06 %	**32 %**
Uend2 PF	0.1 %	0.1 %	0.2 %	0.2 %	0.2 %	**100 %**
Uend2 I	0.08 %	0.06 %	0.05 %	0 %	0.04 %	**1808 %**
Uend2 II	0.1 %	0.2 %	0.2 %	0.2 %	0.2 %	**2575 %**

Foresight until 2030: $T < T^*$

Analogous to the analysis of the Ramsey growth model (Section 4.2), a robust evaluation of the different end-value approaches requires assessing their performance also over a shorter optimization horizon with the system still being in transition.

Figure 13 presents the results for perfect foresight up to 2030, alongside the results for myopic foresight with a horizon ending in 2030.



(a) *Scenario H-PF*

(b) *Scenario H-PF*

(c) *Scenario H-MF-2030*

(d) *Scenario H-MF-2030*

Fig. 13: **Evolution of variables K, Y, C, I, *capacityADD*, and *capacity* in the hybrid model under perfect and myopic foresight. The scenarios are defined in Table 2.** Capacity additions are shown as shaded areas, while total capacity is indicated by the lines. The initial year ($t = 0$) is set to 2025.

Under perfect foresight, the model has not yet reached its steady state: the capital stock K is still increasing (Fig. 13a), and the gas capacity $capacity_{\text{gas}}$ has not yet declined to zero (Fig. 13b). Under myopic foresight, the model is clearly affected by end effects from the start. Investments fall toward zero as early as time step 2026, and capital K continuously declines (Fig. 13c). More strikingly, the model does not invest in generation capacity at all, as indicated by the absence of a shaded area in Fig. 13d.

We now turn to the performance of the various end-value formulations: Figure 14 compares the evolution of K and I_K across different end-value scenarios between 2025 and 2029. The final time step (2030) is omitted, as end values do not perform reliably in the terminal period (see the discussion of Figure 12). Including this time step would visually distort the plot and make it more difficult to assess the earlier dynamics accurately.

The figure shows that each end-value formulation leads to a distinct investment trajectory, which closely mirrors the outcome of the Ramsey growth model. Consistent with the observations from Figure 9, $U^{(1)}_{end}$ leads to slightly higher investment rates, $U^{(2)}_{end}$ with mapping τ_I significantly overinvests, and $U^{(2)}_{end}$ with mapping τ_{II} underinvests relative to the perfect foresight run. Although the plot is truncated at 2029, in 2030 $U^{(2)}_{\text{end}}$ with mapping τ_I also reaches the steady-state capital K^*, consistent with the definition of the mapping presented in Section 3.3.

Figure 15 focuses on the energy-system component of the model. Regarding the investments I_E, the end values generally produce the same trends as observed for I_K. Both $U^{(2)}_{\text{end}}$ with mapping τ_I and $U^{(1)}_{\text{end}}$ result in higher investment rates than the perfect foresight scenario, while $U^{(2)}_{\text{end}}$ with mapping τ_{II} lies between the perfect foresight and purely myopic foresight outcomes.

The plots of investments in coal and gas indicate that $U^{(2)}_{\text{end}}$ with mapping τ_I and $U^{(1)}_{\text{end}}$ invest, similarly to perfect foresight, exclusively in coal, although at slightly higher levels. In contrast, $U^{(2)}_{\text{end}}$ with mapping τ_{II} behaves more myopically, investing only in gas. However, compared to the purely myopic run, it still makes some investments, and is therefore less myopic overall.

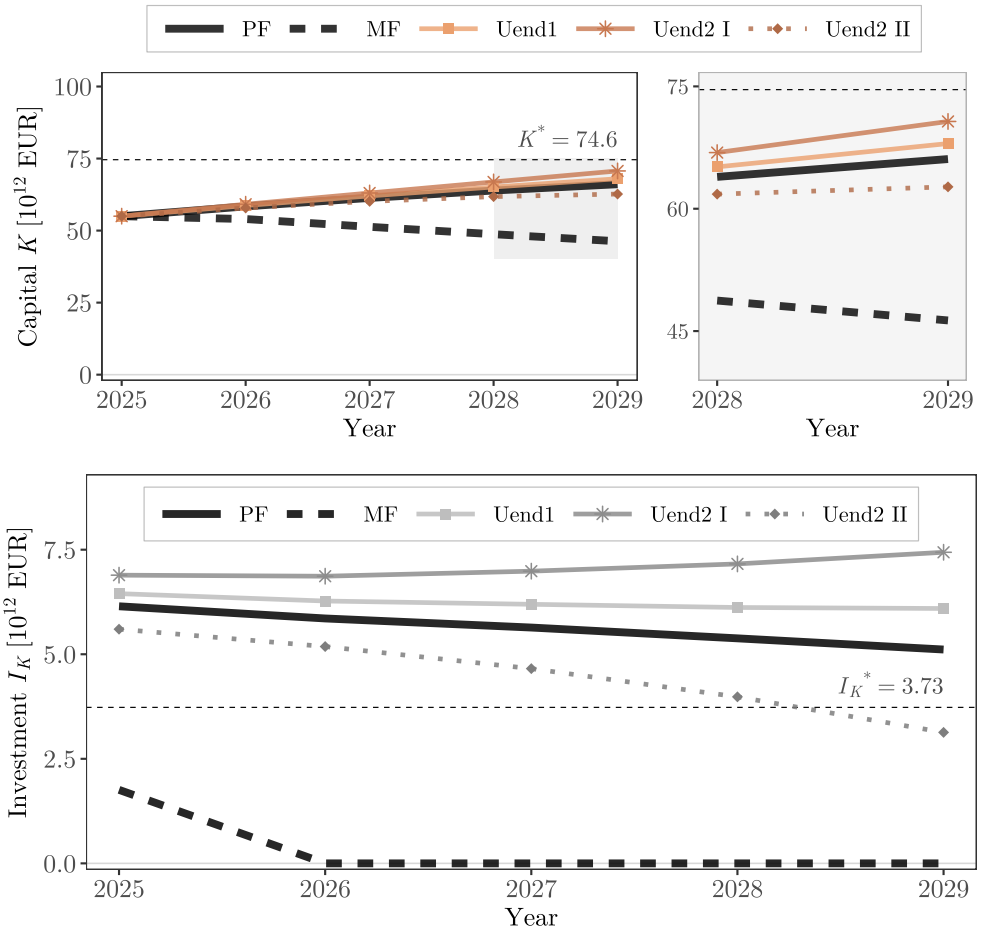


Fig. 14: **Evolution of capital K and investment I_K in the hybrid model under perfect foresight, myopic foresight, and myopic foresight with an end value added to the objective function.** The scenarios shown are *H-PF*, *H-MF-2030*, *H-MF-2030-Uend1*, *H-MF-2030-Uend2-I*, and *H-MF-2030-Uend2-II*. Their definition is provided in Table 2. The initial year ($t = 0$) is set to 2025. Results are shown only up to 2029 to avoid distortions by the final time step (2030).

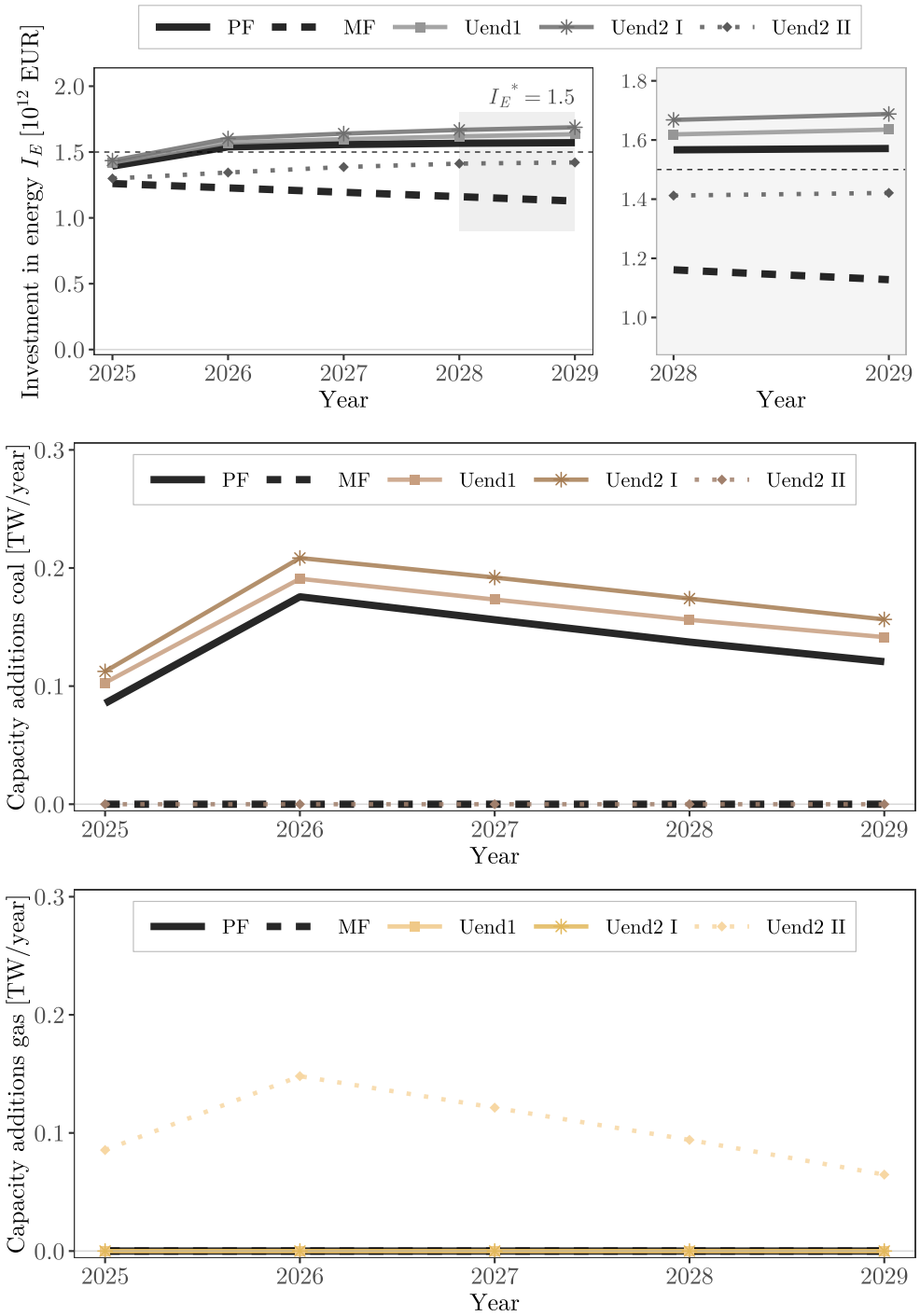


Fig. 15: **Evolution of investment I_E and additions of electricity generation capacity additions** *capacityADD* **in the hybrid model under perfect foresight, myopic foresight, and myopic foresight with an end value added to the objective function.** The scenarios shown are *H-PF*, *H-MF-2030*, *H-MF-2030-Uend1*, *H-MF-2030-Uend2-I*, and *H-MF-2030-Uend2-II*. Their definition is provided in Table 2. The initial year ($t = 0$) is set to 2025. Results are shown only up to 2029 to avoid distortions by the final time step (2030).

5 Discussion and Conclusions

In this study, we presented various end-value formulations that address the finite time horizon problem in hybrid models combining an economic growth model with an energy system model, such as those used in the IAMs DICE (Nordhaus, 1992b), MERGE (Manne et al., 1995), WITCH (Bosetti et al., 2007), or REMIND (Luderer et al., 2015). The performance of these approaches was evaluated using two stylized models: a pure Ramsey growth model and a hybrid energy-economy model. Our main findings are as follows:

Both end value frameworks ($U_{end}^{(1)}$ and $U_{end}^{(2)}$) are applicable not only to the Ramsey growth model but also to hybrid energy-economy models. For optimization horizons sufficiently long for the system to reach its steady state (or balanced growth path), all proposed end value approaches ensure that the finite-horizon solution replicates the infinite-horizon outcome. This property guarantees that deviations observed under shorter horizons arise from transition dynamics or from constraints—such as climate policies or changing fuel prices—that are not fully anticipated within the limited horizon, rather than from a distorted treatment of remaining capital and capacities at the terminal date. Testing end values under long horizons therefore provides a crucial validation benchmark. Although small relative deviations between myopic runs with an end value and perfect foresight runs remain (on the order of 0.2% for the variables I_K and $capacityADD$), we treat these differences as negligible in a numerical context.

For short horizons, end values correspond to different myopic actor types. When the system is still in transition, differences between end values emerge. This demonstrates that the various end-value approaches are not interchangeable; each represents a distinct type of social planner (see Table 1). There are no "right" or "wrong" approaches, but it is important to carefully select the one most suitable for the given case study.

End value $U_{end}^{(1)}$ - *The Pensioner*. This formulation is the only explicit approach; it does not require iterations and consequently offers the lowest computational cost. However, $U_{end}^{(1)}$ yields higher investment rates than the infinite-horizon solution. It can be interpreted as a "pensioner" agent who partially sacrifices present consumption to increase post-horizon utility. This behavior may not align with typical short-term political or private investment decisions, where it is generally expected that investments are lower than in the perfect foresight case. One potential direction for future work would be to introduce a weighting factor in the objective function to balance utility within the planning horizon against utility beyond it. For example, the objective function could be reformulated as $\sum_{t=0}^{T_{MF}} U(C_t) \cdot e^{-\theta t} + \bar{\omega} \cdot U_{end}^{(1)}$ where the weight $\bar{\omega} \in [0, 1]$ represent different degrees of myopia.

End value $U_{end}^{(2)}$ with $\bar{\lambda}_{K,T+1} = \lambda_{K,T+1}^{\infty}$ - *The Clairvoyant's Friend*. This formulation reproduces the exact perfect foresight solution, even under a short horizon.

However, because it relies on shadow prices from a perfect foresight run, it does not represent a genuinely myopic decision-maker. Instead, it serves primarily as a theoretical benchmark. Similarly to the approach suggested for $U_{end}^{(1)}$, future work could explore a formulation where the shadow prices from the perfect foresight run are incorporated into a myopic horizon using a weighting factor applied to the end value.

End value $U_{end}^{(2)}$ with mapping τ_I - *The Overambitious Iterator*. This end value produces the highest investment rates among the approaches considered, resulting in substantial over-investment relative to the perfect foresight solution. By effectively forcing the system toward the steady-state solution early in the horizon, it generates artificial dynamics and is considered the least realistic scenario.

End value $U_{end}^{(2)}$ with mapping τ_{II} - *The Trend-Analyzing Iterator*. This end value is the only one that yields a solution between perfect foresight and purely myopic foresight, which is intuitively the most plausible outcome. Furthermore, the framework itself resembles the behavior of a real-world actor with limited foresight. Consider, for example, an actor with limited foresight: they observe how the value of capital and capacity technologies (reflected in prices or shadow prices) has evolved over the past years and extrapolate that future development will follow a similar trend. Based on this extrapolation, they solve the optimization problem and make their investment decisions. In the following year, they repeat the process, incorporating updated information on the current prices of capital and technologies, and re-extrapolating the shadow prices at the end of the horizon. In a model setting, however, the model does not have access to real-world values and therefore iterates until reaching a consistent development trend of shadow prices. Based on our experiments, one might argue that the results for $U_{end}^{(2)}$ with mapping τ_{II} are "too" myopic. However, it should be noted that we considered an extremely short horizon of only five years. One way to smooth the results—making them slightly less myopic—would be to extend the foresight (e.g., to ten years) and implement a rolling-horizon approach. In this setup, decisions would be made for the next five years while accounting for the subsequent ten-year period.

In hybrid models, the proposed end values do not replicate the infinite-horizon solution in the final time step. This differs from the pure Ramsey growth model and is due to the fact that the hybrid model cannot distinguish between investments in energy capacities and capital occurring in time step T. As discussed in Section 4.3, this depends on the exact formulation of the capital motion and capacity accumulation equations. To overcome this issue, it is important to run the hybrid model with one additional time step beyond the period of interest.

Convergence speed in $U_{end}^{(2)}$ matters. In large IAMs, each iteration may require several minutes or even hours of solve time. While mapping τ_I converges significantly faster than τ_{II}, both typically require more than 20 iterations to reach a relative error below 0.2% (e.g., when assessed for the variable I_K compared to the perfect foresight solution). Currently, no specific start value is chosen, and the convergence process begins from $\bar{\lambda}_{K,T+1|i=0} = 0$. Future work could explore whether convergence

can be improved by selecting a different start value or by assessing whether the time-step length, which is often greater than one year in large IAMs, has an impact on convergence.

For more complex growth dynamics or energy systems, the end-value approaches presented here face certain limitations. All formulations in this study were derived and tested under the assumption of a constant economic growth rate ($g = n$). In more sophisticated models, multiple parameters may evolve over time – including not only labor growth but also efficiency and productivity parameters – and labor growth itself may be non-constant. Such non-linear dynamics would complicate the formulation of $U_{end}^{(1)}$ and $U_{end}^{(2)}$ with mapping τ_I, potentially making an exact analytical derivation infeasible. In these instances, a proxy for aggregate economic growth would be required to maintain the applicability of these end-value formulations. Furthermore, for models featuring more complex energy systems, formulating a meaningful $U_{end}^{(1)}$ can be challenging, particularly regarding the accurate estimation of energy expenditures. In contrast, $U_{end}^{(2)}$ with mapping τ_{II} remains readily applicable in more complex model formulations, as it does not require an exogenously specified economic growth rate.

The theoretical foundations established in this article provide a basis for future research on the impacts of myopic decision-making in a climate policy context. In future work, the proposed end-value formulations could be tested in larger Integrated Assessment Models (IAMs) featuring more complex growth assumptions, detailed representations of the energy system, and relevant policy interventions. Additionally, exploring different initializations and time-step lengths could offer valuable guidance for improving the convergence and stability of the iterative end-value approaches. Finally, implementing a rolling-horizon myopic IAM would enable comparisons between benchmark solutions and trajectories resulting from a myopic social planner. Highlighting the differences between optimal trajectories and those derived from myopic planning – which more realistically reflects real-world decision-making – can provide critical insights into the practical implications of limited foresight and help refine the design of climate policy interventions.

Author contributions *Conceptualization and theoretical framework*: J.S. and G.L. *Study design, Numerical analysis, and visualisation*: J.S. *Supervision*: R.P. and G.L. *Writing - original draft*: J.S. *Writing - review & editing*: J.S., R.P., and G.L.

Funding This research has received funding from the German Federal Ministry of Research, Technology and Space under grant agreement 03SFK5A0-2 (Ariadne) and the European Union's Horizon 2020 Research and Innovation Programme under grant agreement 101183367 (NEWPATHWAYS).

Data Availability The models used in this study, along with all numerical results, are publicly available on Zenodo (https://doi.org/10.5281/zenodo.21496140). The development repository is maintained on GitHub at https://github.com/joanna-sitarz/Ramsey-IAM-end-values.

Declarations

Ethics and consent to participate Not applicable.

Consent for publication Not applicable.

Competing interests The authors declare no competing interests.

Appendix A Ramsey growth model: derivation of end value U_{end} using integrated tail

We start from equation (2.13):

$$U_{end} = \sum_{t=T+1}^{\infty} U(C^*_{T+1}\, e^{g(t-T)})e^{-\theta t}.$$

With $U(C_t) = \ln(C_t)$, we have

$$\begin{aligned} U_{end} &= \sum_{t=T+1}^{\infty} \ln(C^*_{T+1}\, e^{g(t-T)})e^{-\theta t} \\ &= \sum_{t=T+1}^{\infty} \ln(C^*_{T+1})e^{-\theta t} + \sum_{t=T+1}^{\infty} \ln(e^{g(t-T)})e^{-\theta t}. \end{aligned} \tag{A1}$$

Using geometric series properties:

$$\sum_{t=T+1}^{\infty} e^{-\theta t} = \frac{e^{-\theta(T+1)}}{1-e^{-\theta}},$$

we obtain

$$U_{end} = \frac{e^{-\theta(T+1)}}{1-e^{-\theta}} \ln(C^*_{T+1}) + \sum_{t=T+1}^{\infty} \ln(e^{g(t-T)})e^{-\theta t}. \tag{A2}$$

Here, C^*_{T+1} represents consumption in time step $T+1$ assuming the system reached a balanced growth path. As C^*_{T+1} is dictated by the balanced growth path, it is no longer a free decision variable. Equivalently, we can write

$$C^*_{T+1} = Y_{T+1} - I^*_{T+1}, \tag{A3}$$

where I^*_{T+1} is the investment required to maintain the balanced growth path. Similarly, I^*_{T+1} is not a free decision variable but shall be expressed as a function of the capital stock K_{T+1}.

Assuming the economy reached a balanced growth path and is growing at rate g, the capital motion equation reads:

$$K_{T+2} = K_{T+1} \cdot e^g = K_{T+1}(1-\delta) + I^*_{T+1},$$

which implies

$$I^*_{T+1} = K_{T+1}(e^g - 1 + \delta). \tag{A4}$$

Substituting (A4) into (A3), we obtain

$$C^*_{T+1} = Y_{T+1} - K_{T+1}(e^g - 1 + \delta). \tag{A5}$$

Substituting (A5) into the expression for U_{end} yields:

$$U_{end} = \underbrace{\frac{e^{-\theta(T+1)}}{1-e^{-\theta}} \ln(Y_{T+1} - K_{T+1}(e^g - 1 + \delta))}_{\tilde{U}_{end}} + \underbrace{\sum_{t=T+1}^{\infty} \ln(e^{g(t-T)})e^{-\theta t}}_{\text{const.}}. \tag{A6}$$

Since $\arg\max_x f(x) = \arg\max_x f(x) + \text{const.}$, we can redefine U_{end} to:

$$U_{end} = \tilde{U}_{end} = \frac{e^{-\theta(T+1)}}{1-e^{-\theta}} \ln(Y_{T+1} - K_{T+1}(e^g - 1 + \delta)). \tag{A7}$$

This end value formulation has been used, for example, by Mercenier and Michel (1994). Therein, the capital stock K_{T+1} can be calculated using eq. (2.10):

$$K_{T+1} = K_T(1-\delta) + I_T$$

and the production output Y_{T+1} using eq. (2.8) with $Y_{T+1} = f(K_{T+1}, L_{T+1})$.

Appendix B Energy model

B.1 Nomenclature

Table B1 provides a description of all sets, parameters and variables used in the energy system model.

Table B1: Energy model nomenclature (1)

Indices

Symbol	Description
t	Index of time steps, $t \in \{0, 1, 2, \dots\}$
t_{tot}	Index of absolute time steps, $t_{tot} \in \{-T_{init}, -T_{init}+1, \dots\}$
$\tilde{t}, \hat{t}$	Index of relative timesteps, $\tilde{t}, \hat{t} \in \{1, \dots, lifetime_{te}\}$
te	Index of technologies

Parameters

Symbol	Description	Unit
r	discount rate	
α, b	Depreciation parameters	
T	Final time step	
T_{init}	Number of pre-model time steps	
$lifetime_{te}$	Lifetime of technology te	years
$p^{inv}_{t,te}$	Investment cost of technology te in time step t	€$\cdot$ W^{-1}
$p^{OM}_{t,te}$	Fixed O&M cost of technology te in time step t	€$\cdot$ W^{-1}
$p^{fuel}_{t,te}$	Fuel cost associated with technology te in time step t	€$\cdot$ Wh$^{-1}_{\text{fuel}}$
$\omega_{\tilde{t},te}$	Share of capacity of technology te still available $\tilde{t}$ time steps after installation	
ν_{te}	Capacity factor of technology te	
η_{te}	Conversion efficiency of technology te	Wh $\cdot$Wh$^{-1}_{\text{fuel}}$

Variables

Symbol	Description	Unit
$cost_t$	Total energy system costs in time step t	€
$cost^{inv}_{t,te}$	Investment costs incurred for technology te in time step t	€
$cost^{OM}_{t,te}$	O&M costs incurred for technology te in time step t	€
$cost^{fuel}_{t,te}$	Fuel costs incurred for operating technology te in time step t	€
$capacity_{t,te}$	Total capacity of technology te in time step t	W
$capacityADD_{t_{tot},te}$	Capacity addition of technology te in time step t_{tot}	W/year

Variables

Symbol	Description	Unit
$prodSE_t$	Total secondary energy generated in time step t	Wh
$prodSE_{t,te}$	Secondary energy generated by technology te in time-step t	Wh
$demPE_{t,te}$	Primary energy demand of technology te in time step t	$\mathrm{Wh_{fuel}}$
$V_{capacity,T+1}$	Salvage value of remaining capacities after time step T	€

B.2 Equations

The energy system model is described by equations (B1) - (B8).

$$cost_t = \sum_{te}(cost^{inv}_{t,te} + cost^{OM}_{t,te} + cost^{fuel}_{t,te}) \tag{B1}$$

$$cost^{inv}_{t,te} = capacityADD_{t,te} \cdot p^{inv}_{t,te} \tag{B2}$$

$$cost^{OM}_{t,te} = capacity_{t,te} \cdot p^{OM}_{t,te} \tag{B3}$$

$$cost^{fuel}_{t,te} = demPE_{t,te} \cdot p^{fuel}_{t,te} \tag{B4}$$

$$capacity_{t,te} = \sum_{\tilde{t}=1}^{lifetime_{te}} capacityADD_{t-\tilde{t},te} \cdot \omega_{\tilde{t},te} \tag{B5}$$

$$prodSE_t = \sum_{te} prodSE_{t,te} \tag{B6}$$

$$prodSE_{t,te} \leq capacity_{t,te} \cdot \nu_{te} \tag{B7}$$

$$prodSE_{t,te} = demPE_{t,te} \cdot \eta_{te} \tag{B8}$$

with $capacityADD_{t_{tot},te}$ given for $t_{tot} \in \{-T_{init}, \ldots, -1\}$.

Herein, $\omega_{\tilde{t},te}$ described the depreciation of technology te, i.e., the fraction of installed capacity still operational $\tilde{t}$ time steps after installation.

This study uses polynomial depreciation:

$$\omega_{\tilde{t},te} = 1 - (\frac{(\tilde{t}-1)}{lifetime_{te}})^{b}. \tag{B9}$$

B.3 Salvage value

The energy model can also be run as a standalone model. In this case, the secondary energy demand $prodSE_t$ must be provided exogenously, and the objective becomes minimizing total system costs:

$$\min_{capacityADD_{t,te}} \quad (\sum_{t=0}^{T} cost_t \cdot e^{-rt}) - V_{capacity,T+1} \cdot e^{-rT}$$

$$\text{s.t.} \quad (\text{B1}) - (\text{B8}).$$
$$\forall t \in \{0,\dots,T\}$$

Herein, $V_{capacity,T+1}$ denotes the salvage value of remaining capacities at the end of the optimization horizon ($t = T$), representing the remaining value of installed technologies.

$V_{capacity,T+1}$ can be calculated as follows:

$$V_{capacity,T+1} = \sum_{\hat{t},te} capacityADD_{T+1-\hat{t},te} \cdot p^{inv}_{T-\hat{t},te} \cdot \frac{\sum_{\tilde{t}\geq\hat{t}}^{lifetime_{te}} \omega_{\tilde{t},te} \cdot e^{-r\tilde{t}}}{\sum_{\tilde{t}=1}^{lifetime_{te}} \omega_{\tilde{t},te} \cdot e^{-r\tilde{t}}} \cdot e^{r(\hat{t}-1)}. \tag{B10}$$

The formula calculates the salvage value by: (i) identifying the capacity still in operation after time step T, (ii) weighting it by the fraction of its lifetime remaining, (iii) applying discounting to reflect the present value, and (iv) summing over all technologies and past investment periods. The above formulation is, for example, used in the energy system model LIMES (Osorio et al., 2023).

Appendix C Hybrid model: derivation of end value $U^{(1)}_{end}$ using integrated tail

From the derivation in Appendix A, we know that

$$U^{(1)}_{end} = \frac{e^{-\theta(T+1)}}{1-e^{-\theta}} \ln(C^*_{T+1}). \tag{C1}$$

In the case of a hybrid model, consumption C^*_{T+1} can be written as

$$C^*_{T+1} = Y_{T+1} - I^*_{K,T+1} - I^*_{E,T+1}, \tag{C2}$$

where $I^*_{K,T+1}$ and $I^*_{E,T+1}$ denote, respectively, the capital investment and investments into the energy system required to maintain the balanced growth path. Our goal is to express Y_{T+1}, $I^*_{K,T+1}$, and $I^*_{E,T+1}$ as functions of the stock variables K_{T+1} and $capacity_{T+1,te}$.

C.1 $\boldsymbol{Y_{T+1}}$

From eq. (3.3), it follows that

$$\mathbf{Y_{T+1}} = f(K_{T+1}, L_{T+1}, E_{T+1}), \tag{C3}$$

and by eq. (3.8),

$$E_{T+1} = prodSE_{T+1}.$$

As the economy is on a balanced growth path, we assume that installed capacity operates at its full potential. Thus,

$$\mathbf{E_{T+1}} = \sum_{te} capacity_{T+1,te} \cdot \nu_{te}. \tag{C4}$$

C.2 $\boldsymbol{I^*_{K,T+1}}$

By eq. (A5), the capital investment required for balanced growth is

$$\mathbf{I^*_{K,T+1}} = K_{T+1}(e^g - 1 + \delta). \tag{C5}$$

C.3 $\boldsymbol{I^*_{E,T+1}}$

Next we derive a formulation for $I^*_{E,T+1} = f(capacity_{T+1})$. Using equations (B1) - (B4), the total investments into the energy system are

$$I^*_{E,T+1} = cost_{T+1} = \sum_{te} \Big(capacityADD_{T+1,te} \cdot p^{inv}_{T+1,te} + capacity_{T+1,te} \cdot p^{OM}_{T+1,te} + demPE_{T+1,te} \cdot p^{fuel}_{T+1,te} \Big). \tag{C6}$$

Since capacity operates at full potential on the balanced growth path,

$$demPE_{T+1,te} = capacity_{T+1,te} \cdot \frac{\nu_{te}}{\eta_{te}}. \tag{C7}$$

Thus, it remains to relate $capacityADD_{T+1,te}$ to $capacity_{T+1,te}$. Balanced growth implies

$$capacity_{T+2,te} = capacity_{T+1,te} \cdot e^g, \tag{C8}$$

and by eq. (B5),

$$capacity_{T+2,te} = \sum_{\tilde{t}=1}^{lifetime_{te}} capacityADD_{T+2-\tilde{t},te} \cdot \omega_{\tilde{t},te}. \tag{C9}$$

To obtain a closed form for $capacityADD_{T+1,te}$, we assume

$$capacityADD_{T+2-\tilde{t},te} = capacityADD^*_{T+1,te} \cdot e^{g(\tilde{t}-1)} \qquad \forall\, \tilde{t} \in \{1,\dots,lifetime_{te}\}, \tag{C10}$$

which implies that $capacityADD_{t,te}$ reached a balanced growth path already in time-step $t = T+2-lifetime_{te}$. This assumption, however, is in principle inconsistent with the earlier assumption that total capacity $capacity_{t,te}$ reaches equilibrium in time step $t = T+1$. Consequently, some adjustment dynamics are to be expected: the system may require several time steps to converge, and temporary oscillations can occur.

793 Substituting eq. (C10) into eq. (C9) yields

$$capacity_{T+2,te} = \sum_{\tilde{t}=1}^{lifetime_{te}} capacityADD^{*}_{T+1,te} \cdot e^{-g(\tilde{t}-1)} \cdot \omega_{\tilde{t}}$$

$$= capacityADD^{*}_{T+1,te} \cdot \sum_{\tilde{t}=1}^{lifetime_{te}} e^{-g(\tilde{t}-1)} \cdot \omega_{\tilde{t}}. \tag{C11}$$

794 Using eq. (C8),

$$capacity_{T+1,te} \cdot e^{g} = capacityADD^{*}_{T+1,te} \cdot \sum_{\tilde{t}=1}^{lifetime_{te}} e^{-g(\tilde{t}-1)} \cdot \omega_{\tilde{t}}$$

795 which gives

$$capacityADD^{*}_{T+1,te} = capacity_{T+1,te} \cdot \frac{1}{\sum_{\tilde{t}=1}^{lifetime_{te}} e^{-g\tilde{t}} \cdot \omega_{\tilde{t}}}. \tag{C12}$$

Note that for geometric depreciation with $\omega_{\tilde{t}} = (1-\alpha)^{\tilde{t}-1}$

$$\frac{1}{\sum_{\tilde{t}=1}^{lifetime_{te}} e^{-g\tilde{t}} \cdot \omega_{\tilde{t}}} = \frac{e^{g} - 1 + \alpha}{1 - (e^{-g}(1-\alpha))^{lifetime_{te}+1}}$$

$$= e^{g} - 1 + \alpha \quad \text{for } lifetime_{te} \to \infty,$$

which, substituted in eq. (C12), yields

$$capacityADD^{*}_{T+1,te} = capacity_{T+1,te}(e^{g} - 1 + \alpha). \tag{C13}$$

This result mirrors the logic of equation (C5), where $I^{*}_{T+1} = K_{T+1}(e^{g} - 1 + \delta)$. However, as this constitutes a specific limiting case, the analysis will proceed using the general formulation in equation (C12).

Plugging (C12) and (C7) into (C6), we can express the investments into the energy system $I^*_{E,T+1}$ as a function of the stock variable $capacity_{T+1}$

$$\mathbf{I^*_{E,T+1}} = \sum_{te} capacity_{T+1,te}\Big(\frac{p^{inv}_{T+1,te}}{\sum_{\tilde{t}=1}^{lifetime_{te}} e^{-g\tilde{t}}\omega_{\tilde{t}}} + p^{OM}_{T+1,te} + \frac{\nu_{te}}{\eta_{te}} p^{fuel}_{T+1,te}\Big). \tag{C14}$$

C.4 Final expression for $U^{(1)}_{end}$

Combining equations (C1) - (C14), the final expression for the end value is:

$$U^{(1)}_{end} = \frac{e^{-\theta(T+1)}}{1-e^{-\theta}} \cdot \ln\big(Y_{T+1} - I^*_{K,T+1} - I^*_{E,T+1}\big) \tag{C15}$$

with
$$\begin{aligned} Y_{T+1} &= f(K_{T+1}, L_{T+1}, E_{T+1}) \\ E_{T+1} &= \sum_{te} capacity_{T+1,te} \cdot \nu_{te} \\ I^*_{K,T+1} &= K_{T+1}(e^g - 1 + \delta), \\ I^*_{E,T+1} &= \sum_{te} capacity_{T+1,te}\Big(\frac{p^{inv}_{T+1,te}}{\sum_{\tilde{t}=1}^{lifetime_{te}} e^{-g\tilde{t}}\omega_{\tilde{t}}} + p^{OM}_{T+1,te} + \frac{\nu_{te}}{\eta_{te}} p^{fuel}_{T+1,te}\Big) \end{aligned}$$

The derivation presented yields an explicit analytical formulation for the end value in the hybrid model. While simulations throughout this study focus on the no-growth case ($g = 0$), the formula in (C15) remains valid under conditions of economic growth. Two assumptions are worth noting: first, due to depreciation, transitional dynamics — including oscillations — may occur as the system converges to the balanced growth path; second, the formulation assumes that installed capacity operates at full potential, which is reasonable once the balanced growth path has been reached.

Appendix D Hybrid model: derivation of end value $U_{end}^{(2)}$ using shadow prices

D.1 First order conditions of Ramsey growth model

To provide the mathematical background for the shadow price approach, we use the pure Ramsey growth model without a coupled energy system. The finite-horizon problem is formulated as follows:

$$\max_{C_t} \quad \sum_{t=0}^{T} U(C_t)e^{-\theta t} + U_{end}^{(2)}$$

$$\begin{aligned}
\underset{\forall t\in\{0,\dots,T\}}{\text{s.t.}} \quad & Y_t = C_t + I_t \\
& Y_t = f(K_t, L_t) = A_t \left[\xi_K(\mu_K K_t)^\rho + \xi_L(\mu_L L_t)^\rho\right]^{\frac{1}{\rho}} \\
& L_t = L_0 e^{nt} \\
& K_{t+1} = K_t(1-\delta) + I_t \\
& I_t \geq 0 \\
& \text{with } K_0 > 0 \text{ and } L_0 > 0 \text{ given.}
\end{aligned}$$

The Lagrangian for this problem can be written as:

$$\begin{aligned}
\mathcal{L}(C_t, K_t, \lambda_{C,t}, \lambda_{K,t}, \mu_t) = & \sum_{t=0}^{T} [U(C_t)\, e^{-\theta t} + \lambda_{C,t}\big(Y_t - I_t - C_t\big) - \mu_{I,t}\, I_t] \\
& + \sum_{t=0}^{T} \lambda_{K,t+1}\big(K_t(1-\delta) + I_t - K_{t+1}\big) + U_{\text{end}}^{(2)}.
\end{aligned} \tag{D1}$$

The First-order conditions (FOC) are
for $t = 0, \dots, T$:

1. $\frac{\partial \mathcal{L}}{\partial C_t} = \frac{\partial U(C_t)\, e^{-\theta t}}{\partial C_t} - \lambda_{C,t} = 0$
2. $\frac{\partial \mathcal{L}}{\partial K_t} = \lambda_{C,t} \frac{\partial f(K_t, L_t)}{\partial K_t} - \lambda_{K,t} + \lambda_{K,t+1}(1-\delta) = 0$
3. $\frac{\partial \mathcal{L}}{\partial I_t} = -\lambda_{C,t} + \lambda_{K,t+1} - \mu_{I,t} = 0$

   with $\mu_{I,t} \cdot I_t = 0, \quad \mu_{I,t} \geq 0, \quad I_t \geq 0$

in $t = T + 1$:

4. $\frac{\partial \mathcal{L}}{\partial K_{T+1}} = -\lambda_{K,T+1} + \frac{\partial U_{end}^{(2)}}{\partial K_{T+1}} = 0$

D.2 Exact end value using shadow prices

From the last FOC, it follows that at optimum, the shadow price of capital in period $T + 1$ satisfies:

$$\lambda_{K,T+1} = \frac{\partial U_{end}^{(2)}}{\partial K_{T+1}}.$$

If $U_{end}^{(2)} = 0$, then $\lambda_{K,T+1} = 0$, which is consistent with the assumption that capital beyond the horizon has no value in the finite-horizon problem.

To ensure that the finite-horizon solution for $t \in \{0, \ldots, T\}$ coincides with the infinite-horizon solution, the shadow price of capital at $T + 1$ must equal the infinite-horizon shadow price, $\lambda_{K,T+1}^{\infty}$. That is:

$$\frac{\partial U_{end}^{(2)}}{\partial K_{T+1}} = \lambda_{K,T+1} = \lambda_{K,T+1}^{\infty}.$$

A simple choice of the end-value function that satisfies this condition is:

$$U_{end}^{(2)} = K_{T+1}\, \lambda_{K,T+1}^{\infty}.$$

D.3 Note on the hybrid model

An analytical derivation of the iterative approach for the hybrid model is beyond the scope of this work. However, Section 4 shows that treating the salvage value of energy capacity, $V_{capacity,T+1}$, analogously to an additional capital stock delivers excellent numerical performance and closely approximates the infinite-horizon solution. Accordingly, the end value function in the hybrid model takes the form

$$U_{end}^{(2)} = \left(K_{T+1} + V_{capacity,T+1}\right) \cdot \bar{\lambda}_{K,T+1},$$

where the term in parentheses represents the combined terminal asset value.

D.4 Relationship between $U_{end}^{(1)}$ and shadow prices

At first sight, the integrated–tail formulation

$$U_{end}^{(1)} = \frac{e^{-\theta(T+1)}}{1-e^{-\theta}}\, U(C_{T+1}^*)$$

appears conceptually different from the iterative approach that directly imposes shadow price dynamics. However, we can show that

$$\frac{\partial U_{end}^{(1)}}{\partial K_{T+1}} = \lambda_{K,T+1}^*,$$

meaning that the integrated tail approach embeds an implicit assumption about shadow prices: it values terminal capital as if the economy enters a balanced growth path from K_{T+1} onward.

We begin by differentiating $U_{end}^{(1)}$:

$$\begin{aligned}\frac{\partial U_{end}^{(1)}}{\partial K_{T+1}} &= \frac{\partial}{\partial K_{T+1}}\left[\frac{e^{-\theta(T+1)}}{1-e^{-\theta}}\, U(C_{T+1}^*)\right] \\ &= \frac{e^{-\theta(T+1)}}{1-e^{-\theta}}\, \frac{\partial U(C_{T+1}^*)}{\partial K_{T+1}}.\end{aligned}$$

Using the chain rule:

$$\frac{\partial U_{end}^{(1)}}{\partial K_{T+1}} = \frac{e^{-\theta(T+1)}}{1-e^{-\theta}}\, \frac{\partial U(C_{T+1}^*)}{\partial C_{T+1}^*}\, \frac{\partial C_{T+1}^*}{\partial K_{T+1}}. \tag{D2}$$

D.4.1 Derivation of $\frac{\partial U(C_{T+1}^*)}{\partial C_{T+1}^*}$

The FOC for consumption at $T+1$ gives

$$\frac{\partial U(C_{T+1}^*)}{\partial C_{T+1}^*} = \lambda_{C,T+1}^* \cdot e^{\theta(T+1)}.$$

Along the balanced growth path we have

$$\lambda^*_{C,T+1} = \lambda^*_{C,T} \cdot e^{-(\theta+g)} = \lambda^*_{K,T+1} \cdot e^{-(\theta+g)}.$$

Hence, we obtain

$$\frac{\partial U(C^*_{T+1})}{\partial C^*_{T+1}} = e^{-(\theta+g)} e^{\theta(T+1)} \lambda^*_{K,T+1}. \tag{D3}$$

D.4.2 Derivation of $\frac{\partial C^*_{T+1}}{\partial K_{T+1}}$

Using the resource and capital accumulation constraints, we obtain:

$$\frac{\partial C^*_{T+1}}{\partial K_{T+1}} = f'_K(K_{T+1}, L_{T+1}) + (1 - e^g - \delta).$$

On the balanced growth path, the FOC for capital gives:

$$f'_K(K_{T+1}, L_{T+1}) = e^{\theta+g} + \delta - 1.$$

Thus:

$$\begin{aligned} \frac{\partial C^*_{T+1}}{\partial K_{T+1}} &= \left(e^{\theta+g} + \delta - 1\right) - (e^g - 1) - \delta \\ &= e^{\theta+g} - e^g. \end{aligned} \tag{D4}$$

D.4.3 Final formulation

Putting all pieces together, we obtain

$$\frac{\partial U^{(1)}_{end}}{\partial K_{T+1}} = \underbrace{\frac{e^{-\theta(T+1)}}{1 - e^{-\theta}} \cdot e^{-(\theta+g)} \cdot e^{\theta(T+1)} \cdot (e^{(\theta+g)} - e^g)}_{=1} \cdot \lambda^*_{K,T+1} = \lambda^*_{K,T+1}. \tag{D5}$$

This result shows that the end value $U^{(1)}_{end}$ generates a shadow price for terminal capital $\lambda^*_{K,T+1}$ consistent with the assumption of a balanced growth path from K_{T+1} on.

Note, however, that this shadow price does not coincide with the shadow price obtained from the iterative approach with mapping τ_I. While the iterative approach with mapping τ_I reaches the true (infinite-horizon) balanced growth path at time step T, the integrated tail approach defines a hypothetical balanced growth path starting from $T+1$, anchored entirely at K_{T+1}.

Appendix E Parametrization of runs

All parameters used in this study are based on values used in the REMIND (Luderer et al., 2015) and LIMES (Osorio et al., 2023) models for the region Europe. While the purpose of this study isn't to realistically depict the European economy, we still chose parameters ensuring an economy growth and energy system development in a realistic order of magnitude.

Table E1 and E2 provide the parameter values used in the Ramsey growth model and the hybrid model, respectively.

Table E1: Parametrization of Ramsey growth model

Initial values

Symbol	Description	Value	Unit
K_0	Initial capital (in $t = 0$)	50	10^{12} €
L_0	Initial labor (in $t = 0$)	0.3	10^9 people

Parameters

Symbol	Description	Value
A	Productivity factor	1
n	Labor growth parameter	0
ρ	Substitution parameter	-3
ξ_L	Share parameter (labor)	0.6
ξ_K	Share parameter (capital)	0.4
μ_L	Efficiency parameter (labor)	90
μ_K	Efficiency parameter (capital)	0.4
δ	Capital depreciation rate	0.05
θ	Pure rate of time preference	0.03

Table E2: Parametrization of hybrid model

Macroeconomics

Initial values

Symbol	Description	Value	Unit
K_0	Initial capital (in $t = 0$)	55	10^{12} €
L_0	Initial labor (in $t = 0$)	0.3	10^9 people

Parameters

Symbol	Description	Value
A	Productivity factor	1
n	Labor growth parameter	0
ρ	Substitution parameter	-9
ξ_L	Share parameter (labor)	0.465
ξ_K	Share parameter (capital)	0.353
ξ_E	Share parameter (energy)	0.182
μ_L	Efficiency parameter (labor)	60
μ_K	Efficiency parameter (capital)	0.25
μ_K	Efficiency parameter (energy)	8.4
δ	Capital depreciation rate	0.05
θ	Pure rate of time preference	0.03

Energy system

Sets

Symbol	Description	Value
te	Technologies	$coal$, gas

Initial values

Symbol	Description	Value	Unit
$capacityADD_{t,coal}$ for $t < 0$	Capacity additions coal	0.4	TW/year
$capacityADD_{t,gas}$ for $t < 0$	Capacity additions gas	0.025	TW/year

Parameters

Symbol	Description	Value	Unit
r	Discount rate	0.03	
b	Depreciation parameter	3	
$lifetime_{te}$	Lifetime of technologies	50	years
$cost^{inv}_{t,coal}$	Investment cost coal	1.55	10^{12}€ $\cdot$ TW^{-1}
$cost^{inv}_{t,gas}$	Investment cost gas	0.45	10^{12}€ $\cdot$ TW^{-1}
$cost^{OM}_{t,coal}$	O&M cost coal	1.55	10^{12}€ $\cdot$ TW^{-1}
$cost^{OM}_{t,gas}$	O&M cost gas	0.45	10^{12}€ $\cdot$ TW^{-1}
$cost^{fuel}_{t,coal}$	Fuel cost coal	0.056	10^{12}€$\cdot$TWa$^{-1}_{\text{fuel}}$
$cost^{fuel}_{t,gas}$	Fuel cost gas	0.18	10^{12}€$\cdot$TWa$^{-1}_{\text{fuel}}$

Energy system

Parameters

Symbol	Description	Value	Unit
η_{coal}	Conversion efficiency coal	0.4	$\text{TWa} \cdot \text{TWa}_{\text{fuel}}^{-1}$
η_{gas}	Conversion efficiency gas	0.5	$\text{TWa} \cdot \text{TWa}_{\text{fuel}}^{-1}$
ν_{coal}	Capacity factor coal	0.8	
ν_{gas}	Capacity factor gas	0.8	

Appendix F Supplementary information

F.1 Results, Ramsey growth model

Table F1: Relative error $\epsilon_K = \dfrac{K_{PF} - K}{K_{PF}}$

[%]	2075	2076	2077	2078	2079	2080
Uend1	0	0	0	0	0	0.0001
Uend2-PF	0	0	0	0	0	0
Uend2-I	0	0	0	0.001	0.001	0.002
Uend2-II	0.0001	0.0001	0.0001	0.0001	0.0002	0.0002

Table F2: Relative error $\epsilon_{I_K} = \dfrac{I_{K|PF} - I_K}{I_{K|PF}}$

[%]	2075	2076	2077	2078	2079	2080
Uend1	0.001	0.0006	0.0001	0.0004	0.0006	0.0002
Uend2-PF	0.0002	0.0002	0.0004	0.0004	0.0002	0.0003
Uend2-I	0.0002	0	0.0003	0.0008	0.0013	0.0013
Uend2-II	0.0004	0.0003	0.0006	0.001	0.0012	0.0019

F.2 Results, Hybrid model

Figure F1 shows the evolution of energy system capacities using a geometric depreciation of technologies:

$$\omega_{\tilde{t}} = (1-\alpha)^{\tilde{t}-1} \quad \text{with } \alpha = 0.07.$$

Historical capacity additions ($t < 0$) have been set to: $capacityADD_{t,coal} = 0.09$ TW/year and $capacityADD_{t,gas} = 0.012$ TW/year.

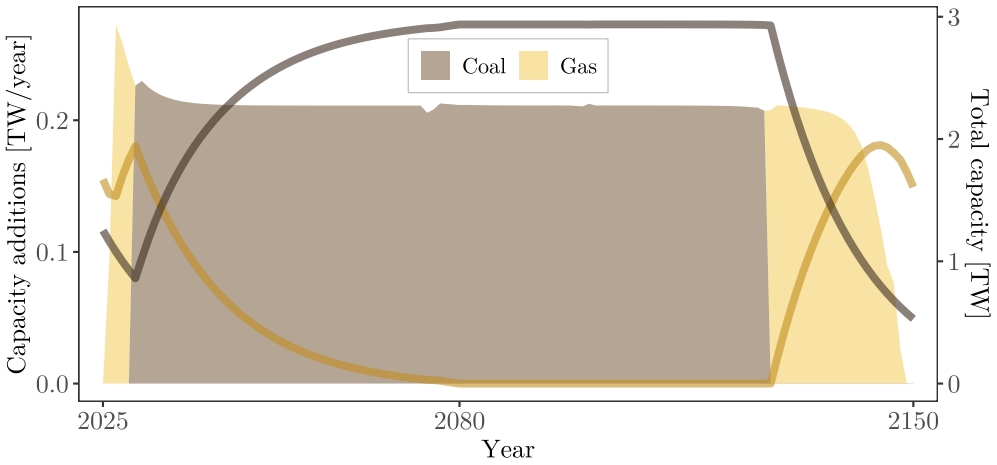


Fig. F1: Extension to Figure 11. Capacity additions (shaded area) and total capacity (lines) of coal and gas under perfect foresight (scenario *H-PF*) with *geometric* instead of *polynomial* depreciation. Geometric depreciation leads to smoother trajectories and removes system oscillations.

Table F3: Evolution of relative error $\epsilon_{K,2080} = \frac{K_{2080|PF} - K_{2080|i}}{K_{2080|PF}}$

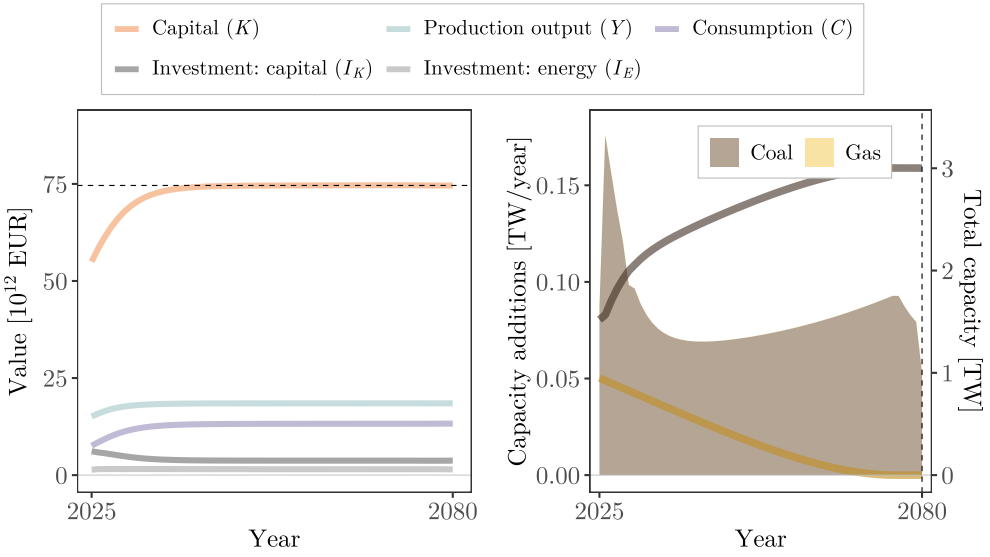
[%]	$i = 0$	$i = 2$	$i = 5$	$i = 10$	$i = 20$	$i = 40$	$i = 60$	$i = 80$
$\mathcal{T}_I$	37	30	18	4	0.3	0.001	0.0002	$\cdots$
$\mathcal{T}_{II}$	37	33	30	24	11	3	0.8	0.2

[%]	$i = 100$	$i = 120$	$i = 140$	$i = 160$	$i = 180$	$i = 200$	$i = 250$	$i = 300$
$\mathcal{T}_I$	0.0002	$\cdots$	$\cdots$	$\cdots$	$\cdots$	$\cdots$	$\cdots$	$\cdots$
$\mathcal{T}_{II}$	0.07	0.02	0.007	0.002	0.001	0.0004	0.0002	0.0002

Table F4: Evolution of relative error $\epsilon_{I_{K,2080}} = \frac{I_{K,2080|PF} - I_{K,2080|i}}{I_{K,2080|PF}}$

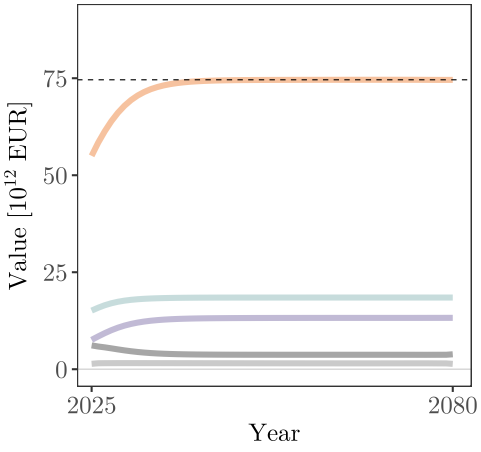
[%]	$i = 0$	$i = 2$	$i = 5$	$i = 10$	$i = 20$	$i = 40$	$i = 60$	$i = 80$
$\mathcal{T}_I$	100	100	100	30	2	0.008	0.003	0.001
$\mathcal{T}_{II}$	100	100	100	100	80	20	6	2

[%]	$i = 100$	$i = 120$	$i = 140$	$i = 160$	$i = 180$	$i = 200$	$i = 250$	$i = 300$
$\mathcal{T}_I$	0.001	$\cdots$	$\cdots$	$\cdots$	$\cdots$	$\cdots$	$\cdots$	$\cdots$
$\mathcal{T}_{II}$	0.5	0.2	0.05	0.02	0.008	0.003	0.002	0.002

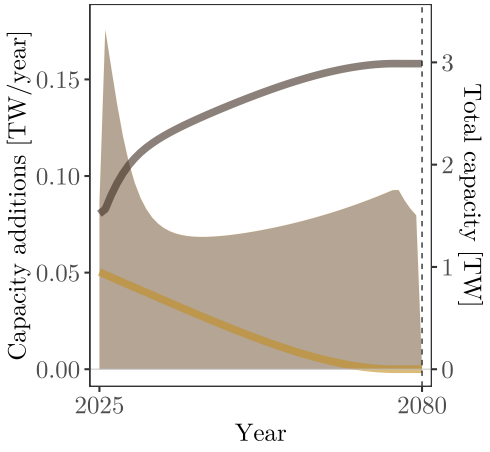


(a) Scenario *H-MF-2080-Uend1*

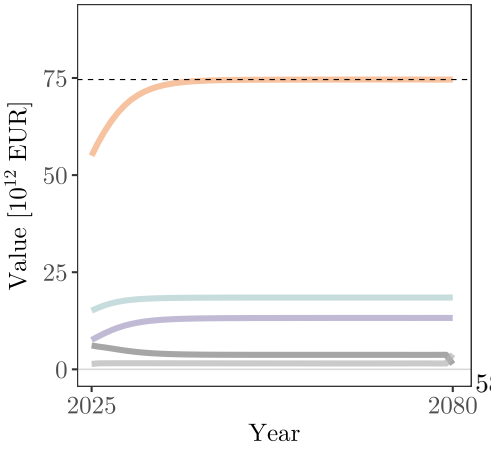
(b) Scenario *H-MF-2080-Uend1*



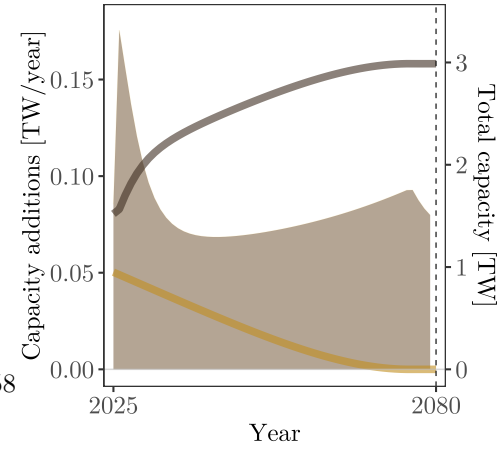
(c) Scenario *H-MF-2080-Uend2-PF*



(d) Scenario *H-MF-2080-Uend2-PF*



(e) Scenario *H-MF-2080-Uend2-I*



(f) *H-MF-2080-Uend2-I*

Fig. F2: **Extension to Figure 12. Evolution of variables K, Y, C, I, *capacityADD*, and *capacity* in the hybrid model under myopic foresight with different end values. The scenarios are defined in Table 2**. The initial year ($t = 0$) is set to 2025. We assume a non-growing economy ($g = 0$).

Appendix G Extension to growing economy

Throughout the main text, results are presented for the case of a non-growing economy. This assumption is made solely to improve visual clarity when illustrating the evolution of model variables and the resulting end effects. It does not affect the applicability of the proposed end-value approaches or the conclusions drawn in this study. In practical applications, integrated assessment models (IAMs) generally include economic growth. Growth may originate, for example, from increasing labor input,

$$L_t = L_0 e^{nt}, \qquad n > 0,$$

or from productivity improvements,

$$A_t = A_0 e^{g_A t}.$$

Furthermore, more complex model formulations may include time-varying efficiency parameters, such as $\xi_{K,t}$, $\xi_{L,t}$, and $\xi_{E,t}$.

The end-value formulations derived in this study assume that the economy converges to a balanced growth path with constant growth rate g, such that, for example,

$$K_{t+1} = K_t e^{g}.$$

The value of g is not imposed exogenously but follows from the underlying growth processes and the model structure. For the CES production function used in this study, labor growth alone implies

$$g = n,$$

whereas productivity growth,

$$A_t = A_0 e^{g_A t},$$

implies

$$g = \frac{g_A}{1-\rho}.$$

When multiple growth drivers are present, the balanced-growth rate is determined by their combined effects.

The model implementation allows for non-zero values of both n and g_A.

Figures G3 and G4 compare the resulting trajectories in a growing economy with $g = 0.01$ under myopic foresight, perfect foresight, and myopic foresight with the end value $U_{end}^{(1)}$.

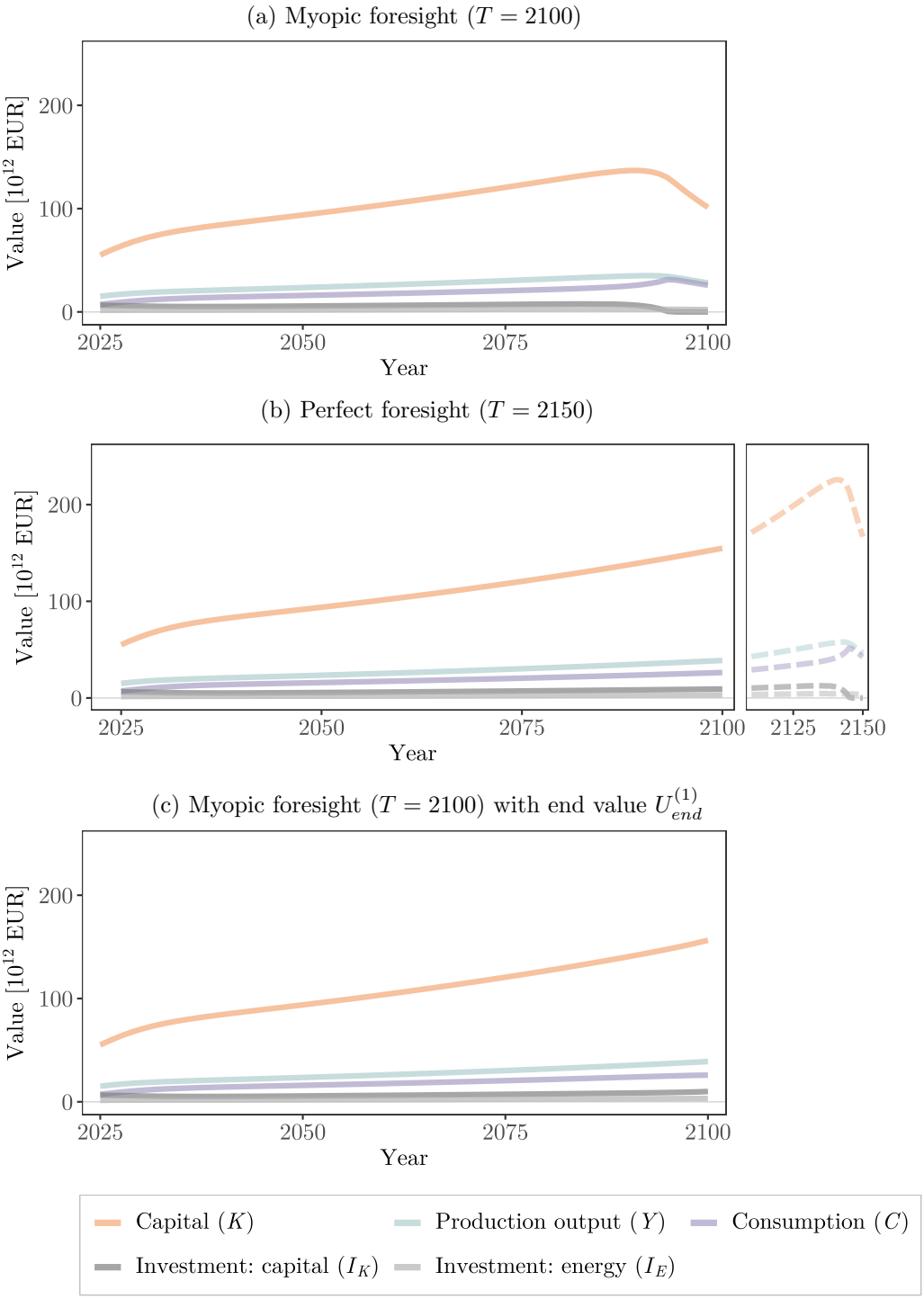


Fig. G3: **Evolution of variables K, Y, C, I_K and I_E in a hybrid model with economic growth ($g = 0.01$).** The initial year $t = 0$ is set to 2025. With an end value $U_{end}^{(1)}$ included in the objective function, end effects are eliminated and the resulting solution closely matches the perfect foresight trajectories.

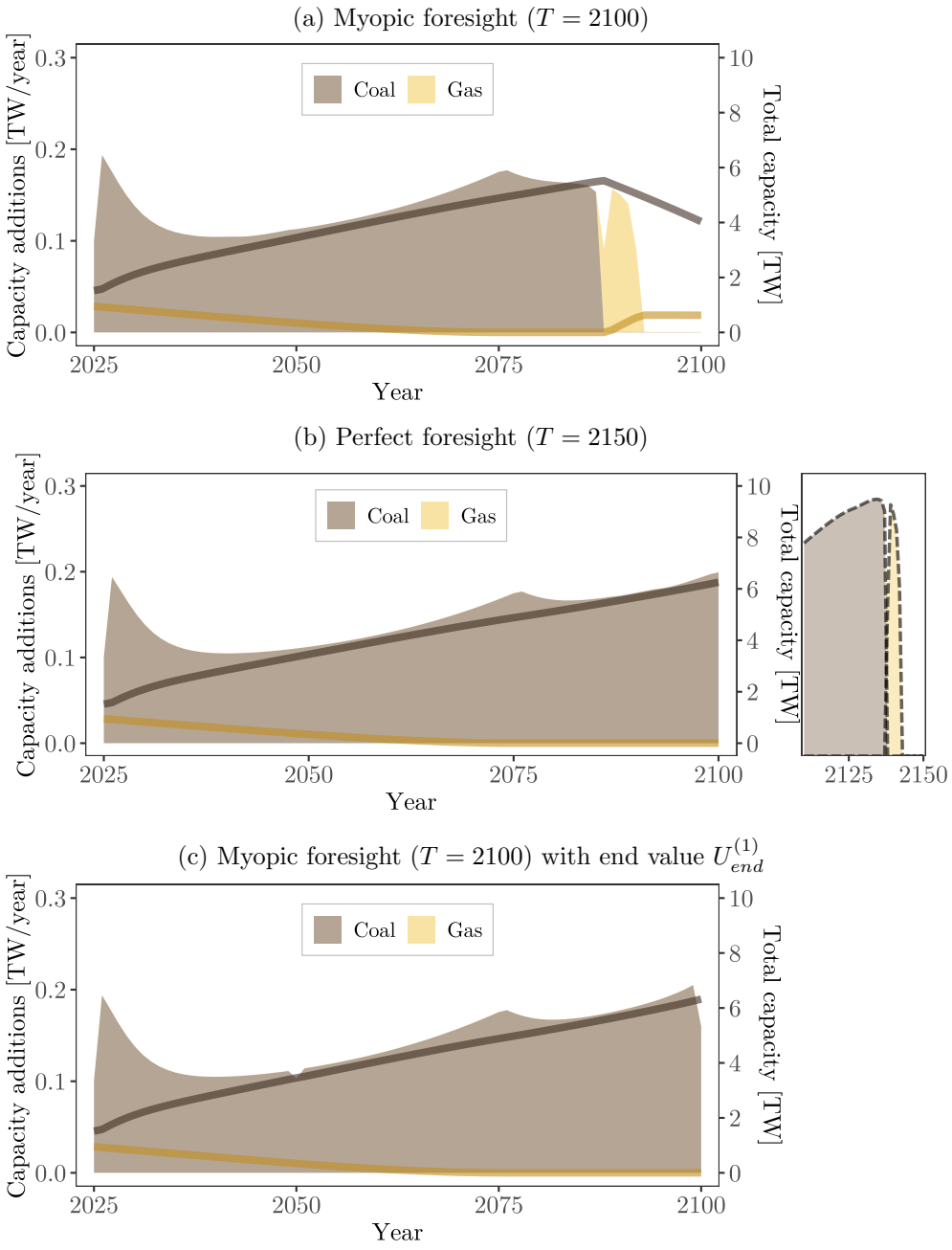


Fig. G4: **Capacity additions (shaded area) and total capacity (lines) of coal and gas in a hybrid model with economic growth ($g = 0.01$).** The initial year $t = 0$ is set to 2025. With an end value $U_{end}^{(1)}$ included in the objective function, end effects are eliminated and the resulting solution closely matches the perfect foresight trajectories.

We show results solely for $U_{end}^{(1)}$, as the corresponding results for $U_{end}^{(2)}$ are qualitatively similar and are available on Zenodo (https://doi.org/10.5281/zenodo.21496141). For more complex growth specifications, however, the performance of $U_{end}^{(1)}$ and $U_{end}^{(2)}$ with mapping τ_I may deteriorate, as these approaches require information about the exogenous growth rate g. In contrast, $U_{end}^{(2)}$ with mapping τ_{II} does not require knowledge of g and is therefore expected to remain applicable under more general growth dynamics.

References

Barr, J.L., Manne, A.S.: Numerical experiments with a finite horizon planning model. Indian Economic Review **2**(1), 1–31 (1967)

Bosetti, V., Massetti, E., Tavoni, M.: The WITCH model: Structure, baseline, solutions. FEEM Working Paper 10.2007 (2007). https://doi.org/10.2139/ssrn.960746 . https://ssrn.com/abstract=960746

Flåm, S.D., J-B., R.: Existence results and finite horizon approximates for infinite horizon optimization problems. Econometrica **55**(5), 1187–1209 (1987) https://doi.org/10.2307/1911267

Fisher-Vanden, K., Weyant, J.: The Evolution of Integrated Assessment: Developing the Next Generation of Use-Inspired Integrated Assessment Tools. Annual Review of Resource Economics **12**, 471–487 (2020) https://doi.org/10.1146/annurev-resource-110119-030314

Guivarch, C., *et al.*: Annex III: Scenarios and Modelling Methods. In: Shukla, P.R., Skea, J., Slade, R., *et al.*(eds.) Climate Change 2022: Mitigation of Climate Change. Contribution of Working Group III to the Sixth Assessment Report of the Intergovernmental Panel on Climate Change. Cambridge University Press, Cambridge and New York (2022). https://doi.org/10.1017/9781009157926.022

GAMS Development Corporation: General Algebraic Modeling System (GAMS) Release 51.2.1. (2025). https://www.gams.com/latest/docs/RN_51.html Accessed 2026-04-15

Grinold, R.C.: Finite horizon approximations of infinite horizon linear programs. Mathematical Programming **12**(1), 1–17 (1977) https://doi.org/10.1007/BF01593765

Krishnan, V., Das, T., Ibanez, E., Lopez, C.A., McCalley, J.D.: Modeling operational effects of wind generation within national long-term infrastructure planning software. IEEE Transactions on Power Systems **28**(2), 1308–1317 (2012) https://doi.org/10.1109/TPWRS.2012.2216293

Kelly, D.L., Kolstad, C.D.: Solving Infinite Horizon Growth Models with an Environmental Sector. Computational Economics **18**, 217–231 (2001) https://doi.org/10.1023/A:1021018417052

Krishnan, V., McCalley, J.D.: Building Foresight in Long-Term Infrastructure Planning Using End-Effect Mitigation Models. IEEE Systems Journal **11**(4), 2040–2051 (2017) https://doi.org/10.1109/JSYST.2015.2410758

Lopes, M.A., Fontes, D., Fontes, F.: Optimal control of infinite-horizon growth models — a direct approach. FEP Working Papers (2015) https://doi.org/10.13140/RG.2.1.5144.4324

Löffler, K., Hainsch, K., Burandt, T., Oei, P.-Y., Kemfert, C., Von Hirschhausen, C.: Designing a model for the global energy system—GENeSYS-MOD: an application of the open-source energy modeling system (OSeMOSYS). Energies **10**(10), 1468 (2017) https://doi.org/10.3390/en10101468

Luderer, G., Leimbach, M., Bauer, N., Kriegler, E., Baumstark, L., Bertram, C., Giannousakis, A., Hilaire, J., Klein, D., Levesque, A., Mouratiadou, I., Pehl, M., Pietzcker, R., Piontek, F., Roming, N., Schultes, A., Schwanitz, V.J., Strefler, J.: Description of the REMIND model (Version 1.6). SSRN Electronic Journal (2015) https://doi.org/10.2139/ssrn.2697070

Lau, M.I., Pahlke, A., Rutherford, T.F.: Approximating infinite-horizon models in a complementarity format: A primer in dynamic general equilibrium analysis. Journal of Economic Dynamics and Control **26**(4), 577–609 (2002) https://doi.org/10.1016/S0165-1889(00)00071-3

Mercenier, J., Michel, P.: Discrete-Time Finite Horizon Approximation of Infinite Horizon Optimization Problems with Steady-State Invariance. Econometrica **62**(3), 635–656 (1994) https://doi.org/10.2307/2951661

Manne, A., Mendelsohn, R., Richels, R.: MERGE: A model for evaluating regional and global effects of GHG reduction policies. Energy Policy **23**(1), 17–34 (1995) https://doi.org/10.1016/0301-4215(95)90763-W

Nordhaus, W.D.: An optimal transition path for controlling greenhouse gases. Science **258**(5086), 1315–1319 (1992) https://doi.org/10.1126/science.258.5086.1315

Nordhaus, W.D.: The 'Dice' Model: Background and Structure of a Dynamic Integrated Climate-Economy Model of the Economics of Global Warming. Cowles Foundation Discussion Papers (1252) (1992)

Osorio, S., Pietzcker, R., Levesque, A., Sitarz, J.: Documentation of LIMES-EU-A long-term electricity system model for Europe. Potsdam Institute for Climate Impact Research (2023). Accessed 2026-04-15

Ramsey, F.P.: A Mathematical Theory of Saving. The Economic Journal **38**(152), 543 (1928) https://doi.org/10.2307/2224098

Wiese, F., Bramstoft, R., Koduvere, H., Alonso, A.P., Balyk, O., Kirkerud, J.G., Tveten, A.G., Bolkesjo, T.F., Münster, M., Ravn, H.: Balmorel open source energy system model. Energy strategy reviews **20**, 26–34 (2018) https://doi.org/10.1016/j.esr.2018.01.003 . Publisher: Elsevier

Weyant, J.: Some Contributions of Integrated Assessment Models of Global Climate Change. Review of Environmental Economics and Policy **11**(1), 115–137 (2017) https://doi.org/10.1093/reep/rew018